SHOCK INDUCED DEGRADATION OF SUPERCONDUCTIVITY IN EXPLOSIVELY FABRICATED BULK METAL - MATRIX COPPER OXIDE HIGH TEMPERATURE SUPERCONDUCTORS

Monu Pradhan-Advani
B. Tech, Inst. of Tech. BHU, Benaras, India

A thesis submitted to the faculty of the

Oregon Graduate Institute
of
Science and Technology

in partial fulfillment of the
requirements for the degree
Master of Science
in
Material Science and Engineering

February, 1990

The dissertation **Shock Induced Degradation of Superconductivity in Explosively Fabricated Bulk Metal-Matrix Copper Oxide High Temperature Superconductors** has been examined and approved by the following thesis committee

Lawrence E. Murr, Professor and Chairman,
Department of Metallurgical Engg.,
University of Texas at El Paso, Texas

Jack H. Devletian, Professor,
Department of Materials Science and Engg.,
Oregon Graduate Institute, Oregon.

Raj Solanki, Associate Professor,
Dept. of Appl. Physics and Electrical Engg,
Oregon Graduate Institute,
Beaverton, Oregon.

This thesis is dedicated to my beloved parents and my husband.

ACKNOWLEDGEMENTS

Thanks are due first and foremost to Dr. L.E. Murr for his guidance, motivation, patience and support during my research work. I would also like to acknowledge Dr. L.H. Schoenline for helping me with my TEM work. Next I would like to express appreciation to my thesis committee, Drs. J.H. Devletian and R. Solanki, husband Dr. Advani, members of faculty and staff and friends C.S. Niou, Dr. U. Sudarsan, Dr. N. Cody, Vivek, Deva and Partha. Finally, thanks to all the people at the center for their continuous encouragement.

This research was supported by the DARPA High-Temperature Superconductivity (HTSC) program through ONR Contract N0001488-C-0684.

TABLE OF CONTENTS

LIST OF FIGURES

ABSTRACT

SHOCK INDUCED DEGRADATION OF SUPERCONDUCTIVITY IN EXPLOSIVELY FABRICATED BULK METAL-MATRIX COPPER OXIDE HIGH TEMPERATURE SUPERCONDUCTORS

Monu Pradhan-Advani, M.S.

Oregon Graduate Institute of Science and Technology, 1990

Supervising Professor: Lawrence E. Murr

Superconducting $YBa_2Cu_3O_7$ and other copper-oxide based superconductors have been successfully encapsulated within a metal matrix by explosive fabrication, however, the residual superconductivity has been found to be degraded. Explosively fabricated powder of $YBa_2Cu_3O_7$ and sintered (98% dense) and shock loaded $YBa_2Cu_3O_7$ exhibit identical systematic changes in residual superconductivity with peak shock pressure. X-ray diffraction studies for explosively fabricated Y-Ba-Cu-O at pressures ranging from 4 to 19 GPa show characteristic split peaks at 2θ = 32 and 58 degrees to be altered systematically with increasing peak pressures, and the midpoint values, (T_c (1/2)) of the resistance-temperature curves decrease with increasing pressure, indicating a broadening of the superconducting transition. The T_c onset does not change between 4 to 8 GPa shock pressure and there is no detectable oxygen loss. Precipitate-like defect clusters associated with

large strain fields, have been observed in the shock processed $YBa_2Cu_3O_7$ by high resolution electron microscopy. This unique localized lattice defect may phenomenologically account for the shock-induced degradation observed in $YBa_2Cu_3O_7$ without any significant orthorhombic-to-tetragonal structure transformation.

CHAPTER 1

INTRODUCTION

The recent revolution in high temperature superconducting materials has generated a wave of intense excitement and activity that has swept through the scientific community attracting the attention of the general public and the news media. The reason being twofold: the unexpected occurrence of superconductivity at such high temperatures is of immense scientific interest, and the new high temperature oxide superconductor may have important technological applications. Recent discovery of superconductivity at temperature up to 95K is one of the more important scientific events of the past decade. The previous understanding has been so fundamentally challenged that a door has been opened to the possibility of room temperature superconductivity. An understanding of the origin and nature of high T_c superconductivity in the new oxide compounds constitutes one of the most important challenging scientific problems that has emerged in recent years.

The new high T_c superconducting oxides hold great promise for technology ranging from large-scale applications involving superconducting magnets, motors, generators and transmission

lines, to small scale applications such as squid magnetometers and digital electronic components based on Josephson junction devices.

CHAPTER 2

BACKGROUND

Superconductivity was discovered by a Dutch scientist, Kamerlingh Onnes, [1] in 1911. He found that the electrical resistance of frozen mercury (Hg) disappeared suddenly at 4.2 degrees Kelvin(K), a temperature accessible only through immersion in liquid helium. Onnes also found in 1913 that weak magnetic fields destroyed the effect, with the metal reverting to its normally resistive state. Subsequently, other metals such as tin and lead were found to be superconductors at similarly low temperatures.

In the 1950's significant progress [5,6] in understanding the physical basis of superconductivity came in. In the theory of Bardeen, Cooper and Schrieffer, interaction leads to a pairing of electrons. At low temperatures the Cooper pairs condense into an electrical superfluid with energy levels a discrete amount below those of normal electron states. [7]

In the years between 1960 and 1986 several hundred materials were found to be superconducting at sufficiently low temperatures. However the highest critical temperature

was 23K in this period, which still required liquid hydrogen cooling or liquid helium.

Recently, new materials have been discovered which have higher T_cs. In January 1986 Bednorz and Mueller [2], working at the IBM laboratories in Zurich and searching for superconductivity in previously unexplored materials, determined that a lanthanum-barium-copper-oxide became superconducting at temperatures over 30K. This unexpected discovery created immense interest in the search for novel materials exhibiting superconductivity at higher temperatures. Later, Chu [3,4] and his colleagues at the University of Houston working with Wu and coworkers at the University of Alabama demonstrated a higher T_c of 90K in Y-Ba-Cu-O system and T_c greater than 100K in BiSrCuO system was announced by Maeda et al [8]. This created a significant impact on the scientific community and it implied that the materials could now be used at temperatures above liquid nitrogen >77K. There have been several preliminary reports of superconductivity at still higher temperatures but at present there is no consensus as to their validity. However room temperature superconductivity would make possible a much broader range of applications.

THEORETICAL UNDERSTANDING

In the microscopic theory of Bardeen-Cooper-Schrieffer (BCS) [7] the presence of a net attractive interaction between conduction electrons, which would normally repel each other because of their like electrical charges, is essential to the occurrence of superconductivity. Conventional BCS theory has two features, one that must be retained by a new theory and one that must be abandoned, or at least supplemented by a new approach. The first is electron pairing; the so-called "Cooper pairs" of BCS theory. It is the second feature, the mechanism of pairing the " glue" that holds the pairs together, that is puzzling to the physicists. In BCS theory the electrons are bound by their interaction with the lattice vibrations of the superconductor which are known as "phonons". There is some evidence that the new materials do not appear to depend on electron-phonon pairing to achieve electron pairing, so theorists have been coming up with other interaction mechanisms.

According to J. Robert Schrieffer the "S" in the BCS theory, the newly emerging mechanisms can be put into three categories. First there are those theories that preserve some aspects of phonon coupling by invoking strong "anharmonic"

effects. The idea is that if normal harmonic vibrating lattice ions do not quite do the job, perhaps vibrations that deviate substantially from harmonicity can cause electrons to interact with greater attraction. In effect if the lattice is not as "stiff" the increased distortion due to the presence of an electron causes a stronger net positive charge, and hence a stronger attraction on other electrons.

The second class of mechanisms involves electric charge fluctuations. In essence, where phonons are ionic lattice vibrations charge fluctuations are the vibrations, of the electrons themselves. If the charge fluctuations can mimic phonons, namely if they can be exchanged back and forth by electrons, then a net attractive force might result.

The third category is that of spin-mediated and magnetic interactions. Electrons not only possess electric charge, but also have "spin" and can act like tiny permanent magnets. A large collection of such spins can experience spin fluctuations and these fluctuations can act as quantized particles that give and take energy from electrons. If conditions are right, electrons can interact through these fluctuations and attract one another.

The appearance of superconducting coherence lengths two orders of magnitude smaller than those previously encountered, the very low carrier concentrations and the apparent importance of both copper and oxygen, will probably require a considerable extension of the current knowledge of superconductivity.

STRUCTURE OF HIGH T_c OXIDE SUPERCONDUCTORS

An understanding of the superconducting mechanism in the newly discovered oxide superconductors is closely connected with a detailed knowledge of the structural properties displayed by these materials. A key to the behavior of the new materials appears to be the presence of planes containing copper and oxygen atoms [9,10,11] chemically bonded to each other. The chemical bonding gives rise to materials that conduct electricity well in some directions in contrast to the majority of ceramics, which are electrically insulating.

The first class of high T_c oxides discovered was based on the chemical alteration of the insulating ternary compound La_2CuO_4 by replacement of a small fraction of the element lanthanum with one of the alkaline earths barium, strontium or calcium. The structure of the superconducting compositions

was studied by x-ray and neutron diffraction [12,13]. The substitution led to compounds with critical temperatures of up to 40K.

In a second class of compounds, based on $YBa_2Cu_3O_x$ the metallic atoms occur in fixed proportions. These are the so-called 1-2-3 compounds which are highly sensitive to oxygen content, changing from semiconducting, at $YBa_2Cu_3O_{6.5}$ to superconducting near 95K at $YBa_2Cu_3O_7$, without losing their crystalline integrity. The substitution of other rare earths even magnetic ones for Yttrium in the 95K compounds results in very little change in superconducting properties. Various materials are under study to understand the present ones as well as to attain higher critical temperatures.

PHYSICAL PROPERTIES

The most important physical properties for applications are the superconducting critical temperature (T_c), the upper critical magnetic field (H_{c2}), the critical current density J_c and the maximum current-carrying capacity in the superconducting state. Also important are the mechanical chemical and electromagnetic properties: physical and thermal

stability, resistance to radiation, and alternating-current.

UPPER CRITICAL MAGNETIC FIELD H_{c2}

Y-Ba-Cu-O samples generally exhibit extremely high upper critical fields [14,15,16]. Preliminary measurements indicate that for single crystals H_{c2} is anisotropic, that is, dependent upon field direction relative to the a-b-or-c axes of the orthorhombic lattice. Values ranging from 30T to 150T are reported at 4.2K. The mechanical stresses associated with the confinement of such high magnetic fields in typical compact geometries are frequently beyond the yield or crushing strengths of known materials. Hence improving these intrinsic H_{c2} values is less important than increasing T_c or J_c values. In fact materials with higher T_cs should exhibit higher H_{c2} values if the performance of known materials that can practically be fabricated into magnets and that retain useful T_cs at field approaching H_{c2} even at 77K is an important change.

CRITICAL CURRENT DENSITY J_c

For practical applications, J_c values in excess of 10^3 amperes per square millimeter are desirable both in bulk

conductors for power applications and in thin film superconductors for microelectronics.

Bulk ceramic conductors of Y-Ba-Cu-O have achieved about 10^3 A/mm^2 at 4.2K and 6T. However, J_c falls off very steeply to levels around 10 A/mm2 at 77K and 6T. There is no clear understanding of these reduced J_c levels, but achieving acceptable values for J_c in bulk high temperature superconductors is of critical importance and must be a principal focus of research on fabrication processes. Preliminary measurements on epitaxially grown single-crystal thin films indicate J_c values in excess of 10^4 A/mm^2 at 77K and Zero magnetic field [17,18]. These values seem adequate for microelectronic applications.

MECHANICAL PROPERTIES

Ceramic high temperature superconductor are very brittle. Hence it may be that high temperature superconductors wire will be wound into magnets prior to the final high temperature oxidation step in its fabrication after which it becomes very brittle. An elastic strain tolerance of 0.5 may be achieved in a multi-filamentary conductor by a fine filament size and by induced compressive stresses. The development of a

mechanical forming process, however, is constrained by the parallel need for the process to optimize J_cs both by aligning anisotropic crystal grains and by increasing the strength of the intergranular electrical coupling.

CHEMICAL STABILITY

The 1-2-3 compounds readily react with the ambient atmosphere at typical ambient atmosphere. These problems seem to be less severe however as the purity and density of the materials are improved. Both water and carbon dioxide participate in the degradation through the formation of hydroxides and carbonates. Further study of the nature of degradation is needed to develop handling procedures or protective coatings that will ensure against impairment of superconducting properties by atmospheric attack.

Chemical stability is also limited because oxygen leaves under vacuum even at room temperature. Surface protection techniques need to be developed to allow satisfactory performance and lifetime of the materials under various conditions of storage and operation. These concerns are heightened in thin films in which for some applications the chemical composition of the outer atomic layers near the surface must be maintained

through many processing steps and in which diffusion into the substrate interface could degrade superconducting properties.

ALTERNATING CURRENT LOSSES

Conventional superconductors exhibit losses in alternating current applications such as in 60 Hertz power transmission or in microwave devices. Although little is known about the alternating current characteristics of the new high temperature superconductors there is no reason to expect that the new materials will exhibit lower alternating current losses than other superconducting materials. Recent measurements on thin films in parallel applied fields show the presence of a large surface barrier for the entry of flux, which indicates that hysteresis losses would be small. More extensive measurements of such losses are required.

SUPERCONDUCTOR FABRICATION

The introduction of ceramic superconductor with $T_c > 90K$ imposes an exciting challenge. As noted above these ceramic oxides are highly unstable, extremely reactive at temperatures above 700C and brittle in nature, and thus difficult to

fabricate in large quantities with a high fraction of the superconducting phase. These limitations presented an opportunity for explosive fabrication as it had been demonstrated [19] that ceramic powders could be efficiently consolidated at reduced processing temperatures by controlling the particle size distribution and peak processing pressure. In addition, Murr et al [20,23] had already shown amorphous metal and other powders could be consolidated and bonded to metal containers.

In the simplest concept it was proposed that explosive powder consolidation could be combined with explosive cladding and welding to produce fully encapsulated conformal superconducting geometries. That is a simple geometry for a superconducting channel could be milled into a metal base plate, filled with a superconducting powder having a requisite size distribution, a cover plate placed over the channel to retain the powder, and a flyer plate or cladding plate arrangement used to consolidate, bond, and clad this conceptual arrangement into a solid monolith-metal or alloy fixture encapsulating a conformal superconducting channel.

Shock waves, which can be conveniently generated by explosives can be characterized in condensed matter as any of three stress waves :

* Elastic waves
* Viscoelastic waves
* Plastic waves

where the material is stressed beyond its elastic limit. W Rankine and H. Hugoniot [24,25] demonstrated that a plastic shock wave or shock front advancing through a material creates a discontinuity in density, pressure, and temperature. This discontinuity advances with a velocity which corresponds to the maximum pressure associated with the shock pulse.

Shock pulses can be generated by rapid displacements resulting from a high velocity impact or an energetic explosion which can produce a compressive velocity of the wave (U_s) and of the mass (U_p) of a compressed material, an equation of state of the material can be determined. Rankine and Hugoniot, actually developed a system of simple equations which in principle describe the conservation of mass (m), momentum(mu), and energy (E) in the high pressure state of condensed matter undergoing shock wave compression.

CONDITIONS AT A SHOCK FRONT

A shock front as depicted ideally and one-dimensionally in Figure 1 [26] propagates through a solid material as a planar shock front which separates the material into two regimes:

* deformed
* undeformed

The disturbance corresponding to the shock front having some finite thickness propagates with a velocity, U_s, called the shock velocity or shock front velocity, into an initially undisturbed or uncompressed state. In the high pressure region behind the shock front, corresponding to the material through which the shock wave or shock pulse has propagated, the material is compressed. Consequently, the regions to the right and left of the shock front (Figure 1) have different densities, specific volumes, and internal energies. The material behind the shock front also moves with a so called particle velocity, U_p, which is different from the shock front velocity. The particle velocity in the undisturbed regime ahead (and to the right) of the shock front, in the so called high pressure region behind the shock front (to the left of Figure 1) the material is compressed, thereby changing the density ($q>q_0$)

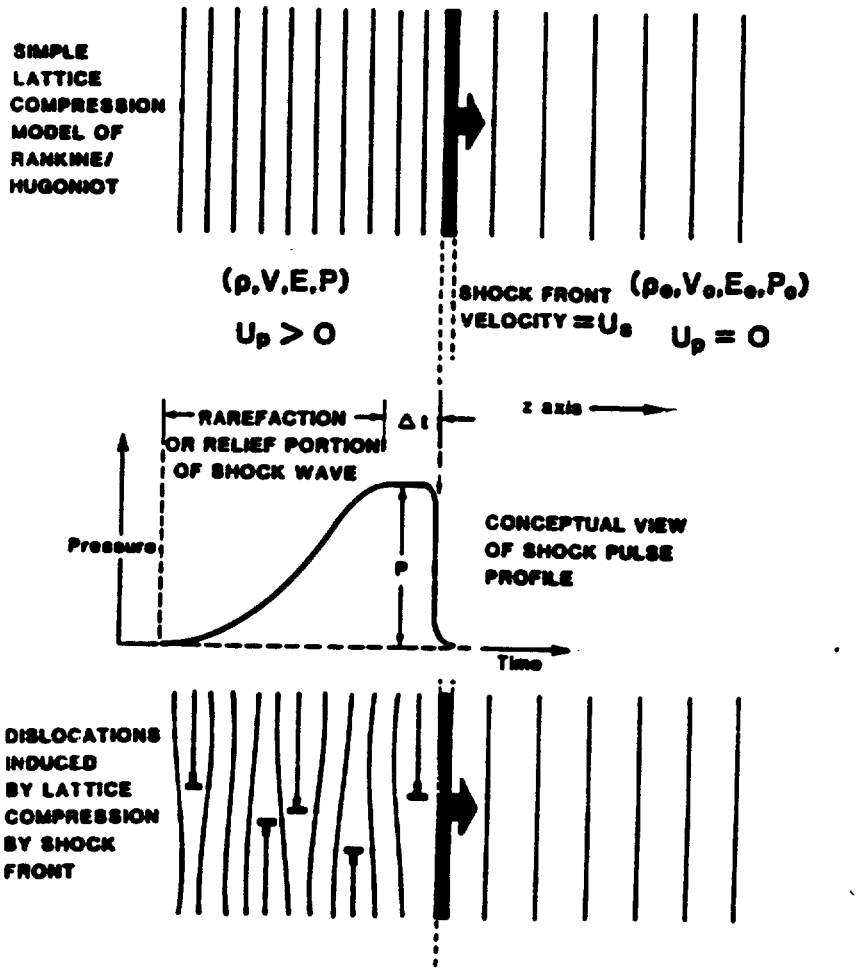

Figure 1 : Schematic representation of two states of condensed matter ahead and behind a propagating shock pulse.

and the internal energy (E > Eo). The material in the shock front also experiences a pressure P (the mean peak pressure) for the shock pulse shown in Figure 1.

Assuming that $P_o = 0$, instabilities in crystalline materials will create dislocations and other crystal defects within the shock front as it propagates.

If a simple system of coordinates is chosen so that the one dimensional system depicted in Figure 1 is at rest at the shock front (z = 0) ; with the shock front propagating in the z-direction), the undeformed or uncompressed material to the right of the shock front can be envisioned to move toward the shock front with a velocity of U_s-U_p. Conservation of mass at the shock front requires that mass entering and leaving must in principle be equal and this can be written in a simple mathematical expression:

$$(U_s-U_p)P = U_sP_o \quad .....(1)$$

Similar for conservation of momentum and energy at the shock front and including Eqn (1) result in the following expressions

$$(P-P_o) = q_o U_s U_p \quad \ldots\ldots\ldots (2)$$

and

$$(E-E_o) = (P+P_o)(V_o-V)/2 \quad \ldots\ldots\ldots (3)$$

where specific volumes

$$V_o = 1/q_o$$

$$V = 1/q$$

The shock velocity and the particle velocity can be expressed by :

$$U_s = V_o[(P-P_o)(V_o-V)]]^{1/2} \quad \ldots\ldots (4)$$

and

$$U_s = [P-P_o]/V_o-V)^{1/2} \quad \ldots\ldots (5)$$

Equations 1-5 are often referred to as the Rankine-Hugoniot equations. Because it is difficult to measure P,V, or certainly E directly for most materials, measurements of the shock velocity, U_s (using electrical or optical methods) described by Rice et al [27] and the particle velocity, U_p, which can be inferred from the so called free surface velocity U_f:

$$U_f = 2U_p$$

serve to establish P and V using Eqns (4) and (5). The resulting Pressure-Volume or P-V data can be plotted as a Hugoniot curve for any given material, and represents the loci of P-V states which are accessible by a shock transition. Simultaneous measurements of U_s and U_p as alluded to above can be used in plotting a Hugoniot curve. Meyers and Murr (28) have more recently also developed a series of Hugoniot tables relating P-V data for a number of materials based on computer solutions of eqns (1) to (5).

Hugoniot curves represent the basic starting point in the design of shock loading experiments or applications or in characterizing a shock or blast wave propagating through a particular material. In a simple flying plate configuration (5) for a plane, compressive shock wave as shown conceptually in Figure 1 the velocity of the flying plate or driver plate, U_d, can be measured by any variety of interruption devices including electrical switches, optical/laser beam switches, etc. Since the driver plate velocity is equal to the free surface velocity, $U_d = U_f$ the particle velocity can be determined using the above equations and the corresponding

peak pressures determined. The actual explosive fabrication process involves two simultaneous processes

* Consolidation of the powder
* Welding of the plates

The above parameters have to be optimized to allow the consolidation of the powder as well as the welding to take place within the constraints imposed by the welding window diagram. The shock wave (and the shock pressure) is of course simultaneously superimposed on this process and is an integral part of this process.

EXPLOSIVE SHOCK WAVE CONSOLIDATION OF METAL AND CERAMIC POWDERS

Shock consolidation of powders is a one stage densification and bonding process which presents potential for consolidation of very hard and difficult to consolidate ceramics. Shock consolidation [29,33] requires the very rapid collapse of the gaps between the particles as well as the rapid deposition of energy at the particle surfaces. These processes need to be close to adiabatic; slow heat transfer to the interior of the particles and surrounding will

radically change the process. This ultra rapid deformation and energy deposition is accomplished in time durations of microseconds of the passage of the shock wave. The selection of shock pressure required to obtain the desired hardness depends on various parameters. The various parameters are :

- initial porosity of powders
- melting temperature
- atomic bonding (metallic, ionic or covalent)
- shape and size of particles
- surface contamination

However hardness seems to be of considerable importance, and is the principal determiner of the needed pressure. This is also related to the residual density achieved in the powder.

The equation of state for the powder is the Mie-Gruneisen equation [28]:

$$P=P_h+ c/V(E-E_h)$$

Where P_h and E_h are the pressure and internal energy of the solid material, P and E are the corresponding values for the powder, and c is the Gruneisen ratio.

EXPLOSION WELDING

Explosive welding can be described in terms of the formation of a fixed joint under high speed contact and interaction of two and more bodies. In practice either a high explosive or sometimes a fine powder charge imparts high speed to one of the bodies being welded. The welding phenomenon takes place within microseconds. If the detonation velocity is below some minimum or greater than the maximum value no welding takes place. Thus the charge height, the height of the cladding plate, the density of the explosive and the distance between the cladding plate and the base plate must be adjusted within the constraints of the welding window diagram.

Thus controlled explosive detonations force two or more metals to bond and weld under high pressures. The time duration involved in the explosive welding event is so small that the reaction zone or heat affected zone (HAZ), between the constituent metals is microscopic. During the process, the first few atomic layers of each metal become plasma due to the high velocity impact [34-37]. Due to the angle of collision this plasma forms a jet in front of the collision point effectively cleaning both surfaces which leaves virgin

metal behind. The remaining thickness of each metal remains near ambient temperature and acts as a huge heat sink which cools the plasma extremely rapidly. The amplitude and the periodicity of the wave pattern formed during explosive welding can be controlled by adjusting three major parameters.

The parameters are explosive load, the explosive detonation velocity and the interface spacing. Thus for a high velocity metal impact, the interface turbulence can be controlled by the explosive detonation velocity and the collision angle.

RESEARCH OBJECTIVE

Measurements of superconductor properties such as resistance-temperature (R-T) curves and current density in explosively fabricated superconducting prototypes have been erratic with current densities measured to be in excess of 10^3 A/cm^2 [22,23,37]. In the present study X-Ray analysis, reduced levitation height measurements and magnetic susceptibility measurements, R-T curves have been used to indicate and quantify degradation in explosively fabricated superconductors. Most of these anomalies and parametric fluctuations may be related to microstructural changes which

depend upon intrinsic phenomenon such as oxygen stoichiometries, crystal phase stability, transformation and strain induced defects. In the present study efforts have been directed towards understanding the cause for this degradation using Transmission Electron Microscopy (TEM). A principal objective involves the effect of shock pressure on the superconducting behavior as measured by the resistance versus temperature (R-T) signature and other simple parameters such as levitation of a standard magnet over uniform samples of fabricated superconductor powder. The superconductor to be investigated consisted of solid state processed $YBa_2Cu_3O_7$ powder [38] or $YBa_2Cu_3O_7$ powder mixed with varying mixtures of copper or silver powders.

CHAPTER 3

EXPERIMENTAL DESIGN

The explosive fabrication and analysis of bulk superconductors involves the following steps :

* Characterization of powder
* Design of Tooling plates
* Plane-wave shock loading
* Optimization of process parameters
* Filling powder into geometries and precompaction
* Extraction of channel geometries from tooling plate
* X-Ray analysis of shocked superconductor
* Levitation height measurements
* R-T curves measurement
* Optical microscopy
* TEM specimen preparation
* Transmission electron microscopy

DESIGN OF TOOLING PLATES

The design of the tooling plates was done by Murr [23]. Figure 2 illustrates a typical experimental design for explosive fabrication of monolithic superconductors. The base plate or matrix was the tooling plate in the fabrication process with the conformal superconducting channels being milled into the base plate. These channels were filled with the superconducting powder and precompacted with a cover plate. The shock wave and the cladding are effected by a flyer or cladding plate. The cover plate is used to pre-compact the powder and acts as a secondary flyer or cladding plate which is welded to the primary and bonded to the consolidated powder channel. In the process the cladding plate is also welded to the base plate. Four series of experiments were conducted. In the first series two assemblies were fabricated one made entirely of copper and the other of silver.

In an effort to improve the process, certain dimensional modifications were introduced in the Series 2 tooling plate design. Two assemblies were made both of copper metal and a provision was made to facilitate evacuation of the milled channels.

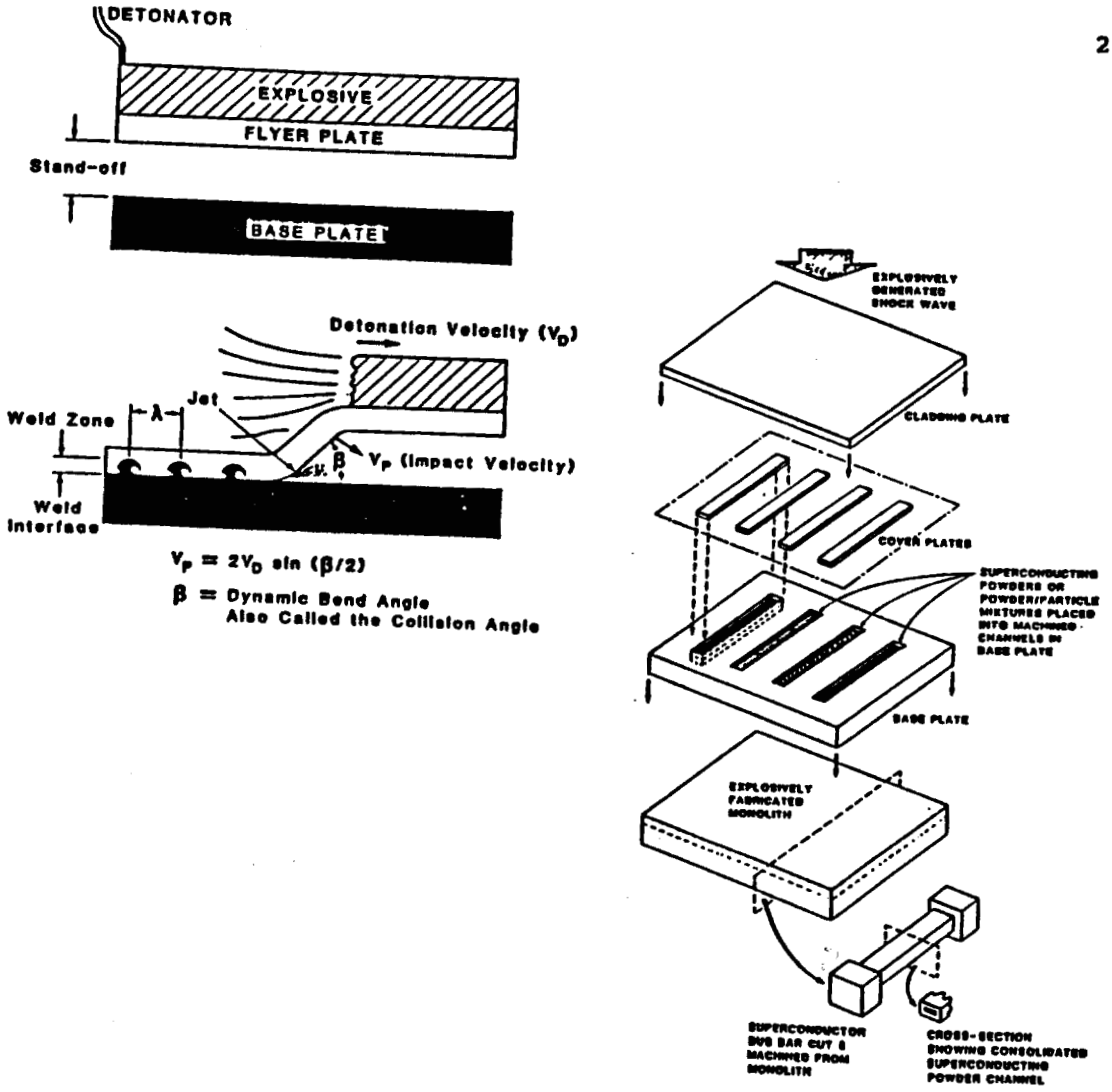

Figure 2 : Arrangement of the superconducting metal matrix for explosive fabrication, plate welding and superconductor consolidation.

In Series three, six assemblies were fabricated and in three of these assemblies a portion of one tooling plate was evacuated while the mating plate had no vacuum provisions. All the six assemblies were made of copper.

In Series four three assemblies were fabricated all made of copper. No provision for evacuation was provided in this series of experiments. However process parameters were modified.

PLANE WAVE SHOCK LOADING

Sintered materials could be subjected to a plane shock wave. The sintered bars were obtained from AT&T Bell Laboratories in Murray Hill, New Jersey. A density compatible assembly Figure 3 was designed to accommodate sintered $YBa_2Cu_3O_7$ bars (98% dense) and $YBa_2Cu_3O_7$ + 25 weight percent Ag bars. The mean density for these samples was 6.8 g/cm^3 and a Zn-5% Al, 2% Cu was developed and cast into plates having a bulk density of 6.7%. From these plates, a plane wave shock assembly was machined and assembled as shown in Figure 3. The experiment illustrated was designed to produce a peak pressure of approximately 6 GPa. The flyer plate thickness was 0.64 cm.

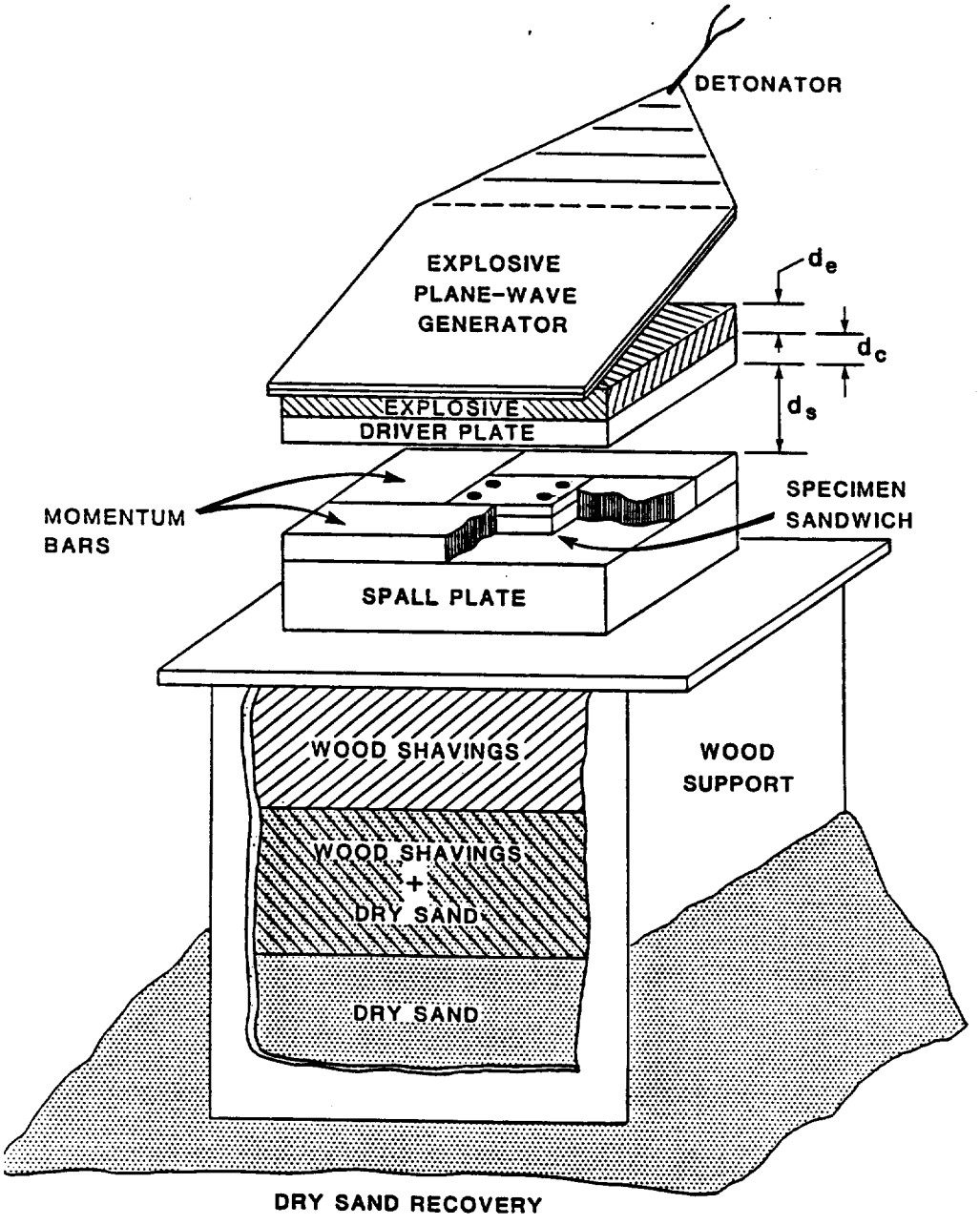

Figure 3 : Schematic arrangement for recovery of density compatible specimen sandwich containing sintered $YBa_2Cu_3O_7$ superconductor samples following plane-wave shock loading

This experiment has been described in detail by Murr et al [39] and is included here as a reference or basis to compare the effects of shock pressure on the explosively fabricated powders.

OPTIMIZATION OF PROCESS PARAMETERS

The explosive fabrication process of bulk superconductors involves two simultaneous processes

* Consolidation of the powder
* Welding of the plates

Figure 4 illustrates the various parameters and the equations involved. The optimization of these parameters was done by Murr. The process parameters were interrelated and affected the process critically as demonstrated in Figure 4a which illustrates the assumptions made in calculating the peak shock pressure in the superconducting powder channels.

The process parameters are listed below

* Type of explosive
* Explosive thickness (d_e)
* Detonation velocity (V_d)
* Cladding plate thickness (d_c)
* Base plate thickness
* Stand off distance (d_s) (This is the distance between cladding plate and base plate)
* Plate velocity (V_p) see Figure 4b
* Peak pressure generated (P_{sc}) see Figure 4b
* Density of the explosive
* Gurney energy E
* Beta (the bend angle also called the collision angle)

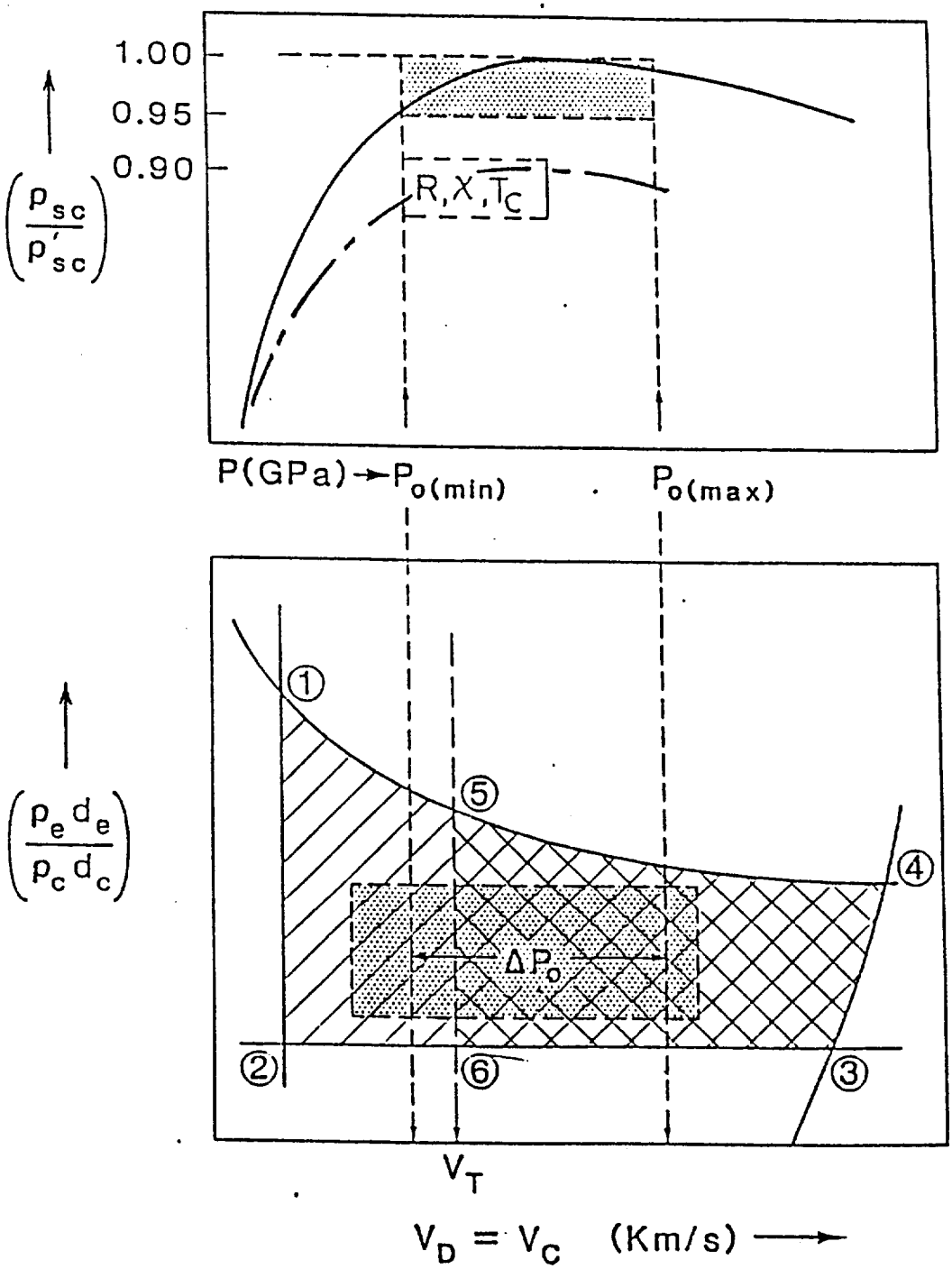

Figure 4a: Idealized views for optimized powder consolidation process based on the superconductor density (qsc) achieved (top) and the optimization of the explosive welding process (bottom).

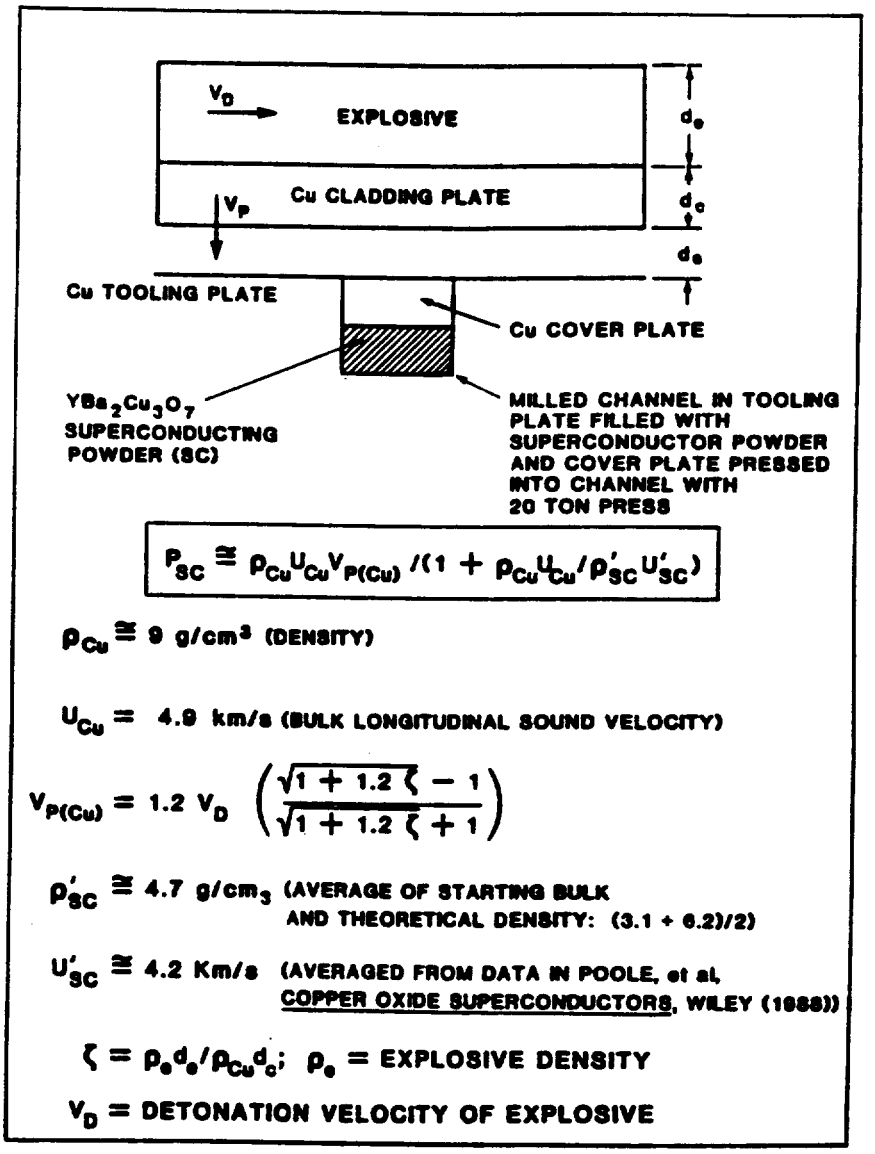

Figure 4b: Experimental approximations for calculating the peak pressure in the superconducting powder during explosive fabrication.

It was particularly important to make reasonable calculations such that the impact pressures and the peak pressure in the channel could consolidate the superconductor powder to assure a requisite final density. Also the process parameters had to be optimized within the constraints of the welding window (Figure 4a).

In Series 1 the peak pressure was 6 GPa for the silver tooling plate design and for the copper 7 GPa (Figure 4b). In the second series the base plate thickness, tooling plate dimensions, stand off distance, cladding plate thickness, plate velocity, and the peak pressure were changed. The peak pressure was 9 GPa.

In the third series of experiment the tooling plate dimensions, and the base plate thickness was reduced, cladding plate thickness was decreased. The detonation velocity and the peak pressures for the six assemblies are enlisted below.

Series 3	Detonation Velocity (Vd) Km/sec	P Pressure(GPa)
Cu(1.1)	1.8	8
Cu(1.2)	1.8	8
Cu(2.1)	2.4	13
Cu(2.2)	2.4	13
Cu(3.1)	2.9	19
Cu(3.2)	2.9	19

In the fourth series of experiments the stand off distance was further reduced and the density of explosive changed. The detonation velocity and the peak pressures are as follows.

Series 4	Detonation Velocity (Vd) Km/sec	Peak Pressure(GPa)
Cu(4.1)	1.8	4
Cu(4.2)	1.8	5
Cu(4.3)	2.0	7

The detonation velocities were determined from the specific composition of ammonium nitrate explosive mixtures (ANFO- ammonium nitrate + fuel oil) [28]. The peak pressures were then calculated as shown in Figure 4b.

POWDER CHARACTERIZATION

Characterization of the superconducting powder was an important feature in the explosive fabrication process. For the final product to be a good superconductor it was essential for the initial, starting powder to have a high fraction of pure superconductor. Superconductivity is found to be limited by the formation of non-superconducting phase or low coherence length on the grains. These powders are highly vulnerable and react to form non-conducting phases which inhibits continuity.

Thus such surface products were a primary concern as illustrated schematically in Figure 5.

The quality of the powder 'good' or 'bad' was judged by conducting levitation height measurements and susceptibility measurements which were inconsistent. The x-ray spectrum of the starting powder revealed characteristic orthorhombic split peaks at $2\theta = 32$ and 58 degrees. Different powders exhibited changes in the split peak signatures and agreed well with the results obtained from levitation height measurements. The X-ray signatures were also observed to vary in systematic ways with variations in fabrication parameters, particularly the peak shock pressure, P_{sc} (Figure 4b).

PRECOMPACTION

The superconducting powder $YBa_2Cu_3O_7$ was prepared by a solid state route described previously [38] and finely ground in a mortar with a pestle with gentle strokes. This powder is then filled into the conformal channel geometries milled into the base plate. The cover plate was then hammered and pressed using a 40 ton static press to fit into the channels to precompact the powder. The tooling plates were then milled to obtain a smooth surface finish. The tooling plate was now ready to be shocked.

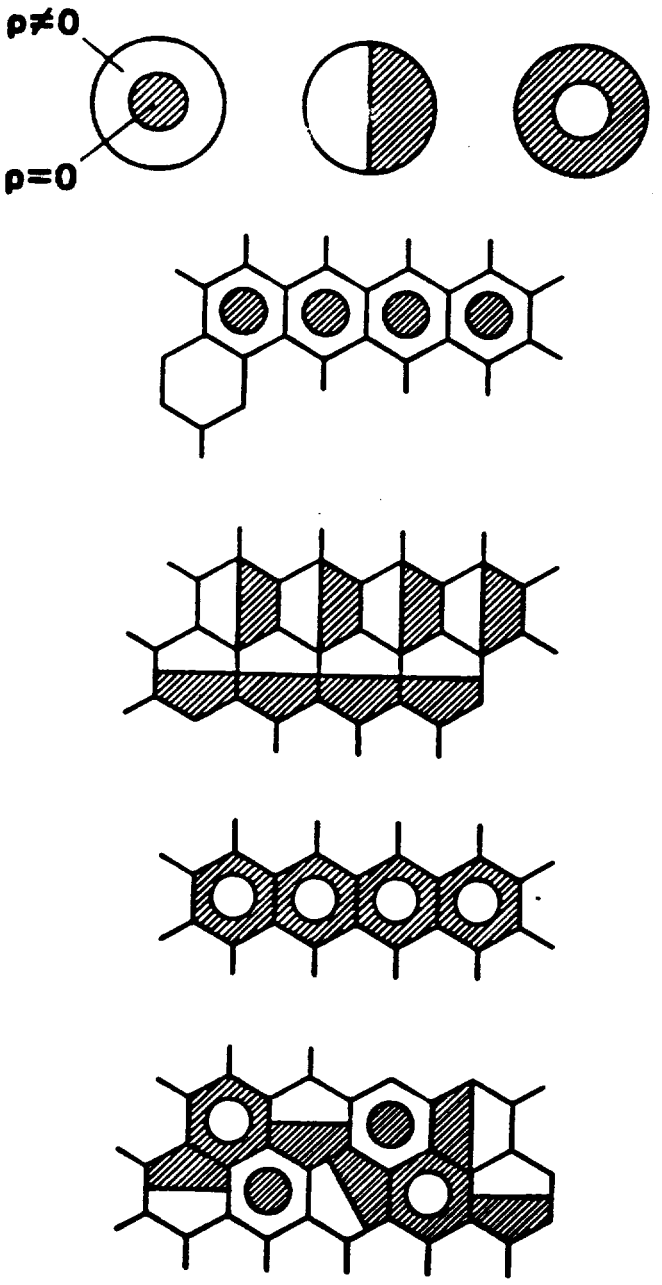

Figure 5 : Simple Microstructures and Phase fraction geometries in the starting Superconductor Powders can have an important influence on the supercurrent transport properties.

X-RAY DIFFRACTION

After explosive fabrication the channel geometries were extracted from the tooling plates. Small sections were cut from the linear geometries encapsulating the superconducting powder taking great care that no heating occurs while cutting. To facilitate the extraction of the consolidated powder from the metal matrix the copper metal was cut from all four sides using a diamond saw which enabled to keep the temperature as low as possible. The resulting superconductor is stored in dessicant bags to prevent exposure to the atmosphere. Extreme care has to be taken to prevent degradation of the superconductor by exposure to air. The superconductor is then ground to a fine powder in a mortar using a pestle. The fine powder is then spread on the glass plate and a run executed on an X-Ray machine to obtain the x-ray spectrum.

A systematic study of the X- Ray spectrum was done on the shocked, unshocked and sintered samples.

TEM SPECIMEN PREPARATION

The three major techniques for preparing thin specimens of $YBa_2Cu_3O_7$ and other ceramics for high resolution electron

microscopy are grinding, cleaving, and ion milling. Artifacts can be introduced by these different techniques. It is concluded that the most serious problem encountered during high resolution electron microscopy studies is a surface initiated decomposition leading to the ultimate degradation of the structure.

The Y-Ba-Cu-O superconductors are highly reactive on exposure to air as well as to water. For Transmission Electron Microscopy thin films of thickness less than 12 mm were required. The superconductor was first ground by a Gatan disc to 30-40μm using methanol, first on 600 grid paper and then on 10, 3, 0.1μm Alumina paper. The specimen glued on the gatan disc is then transferred to a container lined by a filter paper containing acetone. As a consequence the thin specimen falls on the paper which is carefully taken out and the specimen glued on a holey copper disc. The specimen is directly transferred and ion milled at 6 KV with a take off angle of 15 degrees.

After ion milling the specimen is directly transferred to the Transmission electron microscope without delay as the sample decomposes if exposed to air or stored in an evacuated desiccator.

OPTICAL MICROSCOPY

As a consequence of explosive welding the cladding plate and the base plate are explosively bonded. A section of this interface was taken polished and etched. The etchant used for copper interface was 33% sulfuric acid, 33% acetic acid and 34% ammonium hydroxide. The etched surface was observed under the optical microscope.

LEVITATION HEIGHT

Levitation height measurements were made by pressing a disc (for original powder). After explosive fabrication the superconductor is extracted from the encapsulating metal matrix. The disc and the superconductor were cooled in liquid nitrogen and a magnet placed on the disc and the shocked superconductor. The magnet is levitated above the disc and the distance between the magnet and the disc called the "levitation height" was measured.

R-T CURVES

The peak broadening and peak height reductions observed in the x-ray split peak signatures indicated degradation of the superconductor. It was also noted with increase in peak pressures degradation increases. This was confirmed by the R-T curves. The plot of resistance-Temperature yielded curves that revealed degradation and semiconducting behavior of the shocked superconductor. The shocked superconductor was extracted from the encapsulating monolith and a four probe silver contact method used to measure the electrical resistance. A measuring current of 10 mA was usually employed in a specially designed cryostat.

MICROSTRUCTURAL OBSERVATIONS

High resolution electron microscopy was carried out in a Hitachi-800 electron microscope, equipped with a side entry +/- 40 degrees double tilt goniometer operating at 200 kV. The samples were ion beam thinned using an Ar beam at 6 kV and incident angles of 12-14 degrees.

CHAPTER 4

RESULTS AND DISCUSSION

The degradation in superconductors was observed using

* X-ray diffraction
* Levitation height measurements
* Resistance-Temperature curves

OPTICAL OBSERVATIONS

The explosive consolidation of bulk superconductors consists of two processes

* Welding of the plates
* Consolidation of the powder

Explosive welding, is a solid state welding which uses controlled explosive detonations to force two or more metals together at high pressures. The time duration involved in the explosive welding event is so small, that the reaction zone or heat affected zone between the constituent metals is

microscopic. During the process, the first few atomic layers of each metal become plasma due to the high velocity impact. Due to the angle of collision, this plasma jets in front of the collision effectively cleaning the surfaces leaving virgin metal behind. At the bond line, the interface between the base plate and the cladding a wave pattern is formed as illustrated in Figure 6a. The amplitude and periodicity of the wave pattern formed during explosive welding can be adjusting by controlling the welding parameters as shown in Figure 6b the welding window diagram.

X-RAY DIAGNOSIS

After shock the consolidated superconductor was ground to the same size fraction to facilitate comparison between the starting and consolidated powder by maintaining identical particle distribution size and also in effort to eliminate any texturing or other fabrication artifacts.

The split peaks at $2\theta = 32$ and 58 degrees were carefully and systematically studied. In Series 1 the x-ray split peak signatures $2\theta = 32$ exhibited peak height reductions and peak broadening when compared with the x-ray spectrum of the

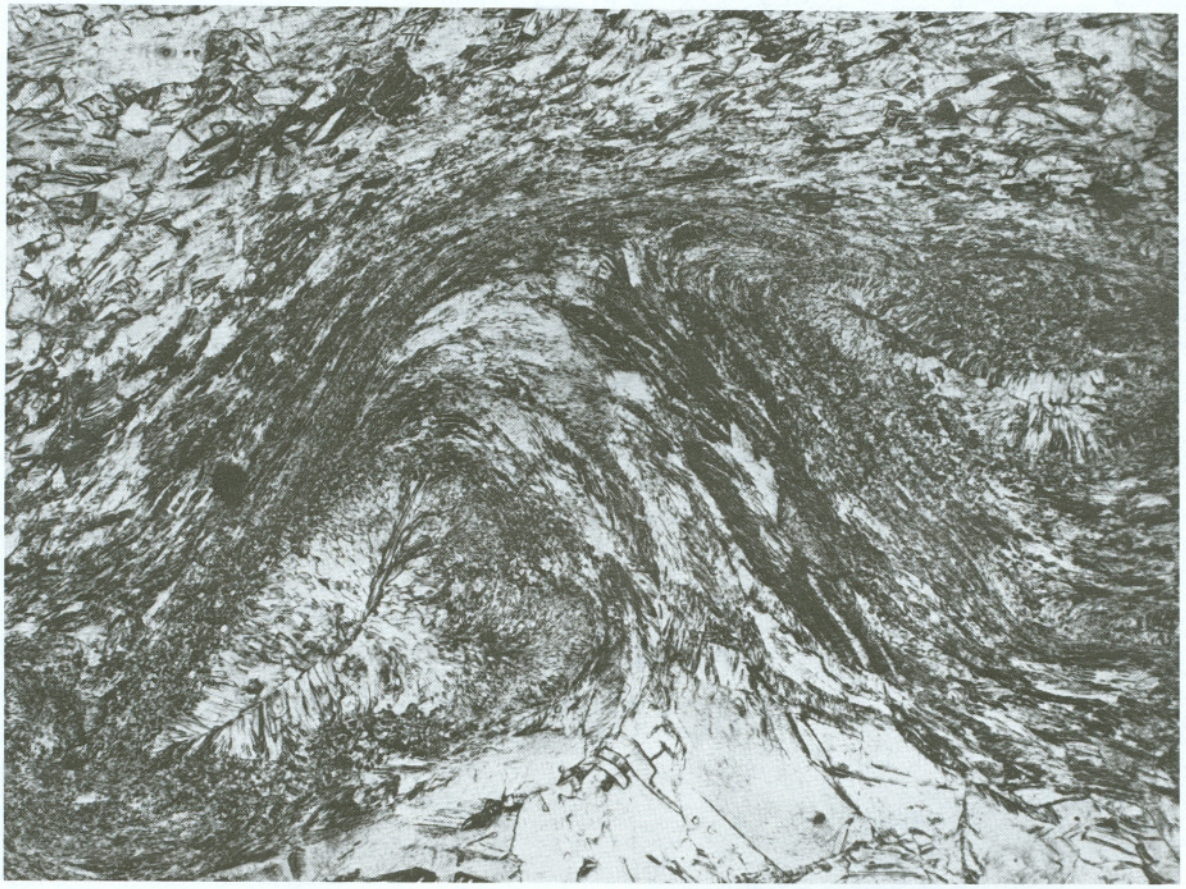

Figure 6a: Weld wave structure observed by optical metallography. The large grain size regime (dark) is the base plate, the other (light) is the tooling plate

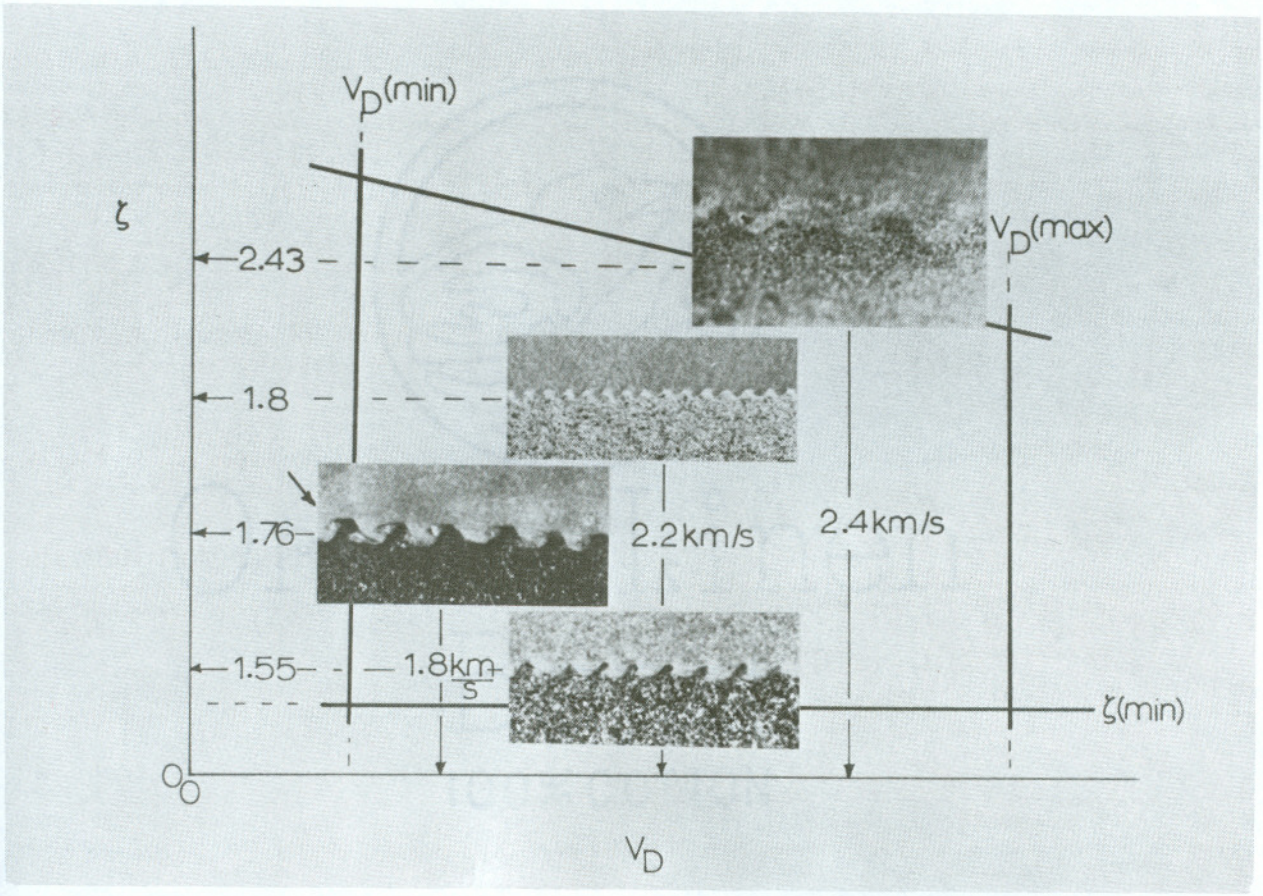

Figure 6b: Experimental features of a welding window diagram for the copper tooling plate explosive welding

starting powder as illustrated in Figure 7. In Series 1 two tooling plates were shocked one made of copper and the other made of silver metal. In this series in addition to the pure superconductor some channels were filled with metal powder and superconductor mixtures to study the effect of metal powder additions on superconductivity, mechanical properties, electrical contact phenomenon and oxygen stabilization.

The % of metal powder additions for copper and silver tooling plates were

Ag TOOLING PLATE	Cu TOOLING PLATE
SC+10% Ag Powder	SC+10% Cu Powder
SC+20% Ag Powder	SC+20% Cu Powder
SC+30% Ag Powder	SC+30% Cu Powder
SC+10% AgO Powder	SC+30% Ag Powder

To make this analysis more effective in terms of the product-performance-superconductivity the degradation and simple superconducting behavior required some quantification data. Quantification of this peak was done by measuring the area of the 32 degree peak designated A(013) and the area

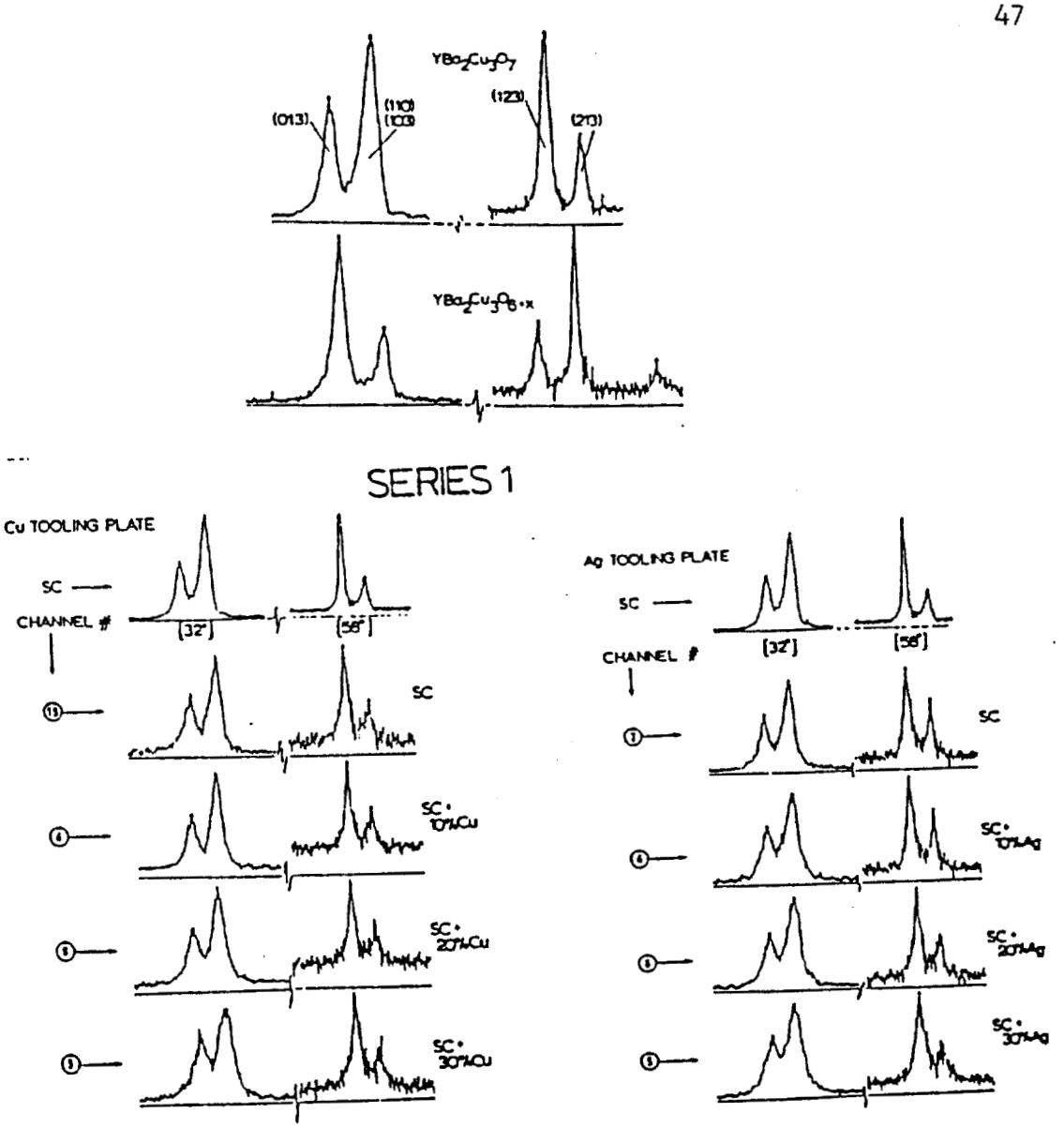

Figure 7 : Details of the x-ray split peak signatures are shown from explosively fabricated experiment denoted Series 1 and of the starting powder. SC denotes the $YBa_2Cu_3O_7$ and when not associated with a channel number represents the unconsolidated powder.

A_t the total area of the split peak for the shocked sample. Similarly the area A and the total area A_t were found for the starting powder. A divided by A_t for the shocked and the starting powder were calculated and the percentage degradation of the superconductor was determined.

In the first series it was observed that as the percentage of metal additions increased the degradation also increased, although 10% metal additions revealed minimal degradation. Both silver and copper tooling assemblies indicated the same results. The degradation of superconductor with 10% metal Ag and Cu powder additions exhibited less degradation. The channels in Series 1 were extracted and a standard (4 mm) magnet levitated over these samples (at 77K). The levitation height H_L was measured from the bottom of the magnet to the top of the superconductor or mixture. These results are shown in Figure 8a and b.

The x-ray analysis of Series 1 experiments invoked modifications in an attempt to consolidate the superconductor without degrading it. There was a possibility that the gases could be trapped within the channel and this could cause degradation. The fabrication parameters were adjusted and two tooling plates were fabricated both of copper. For comparison

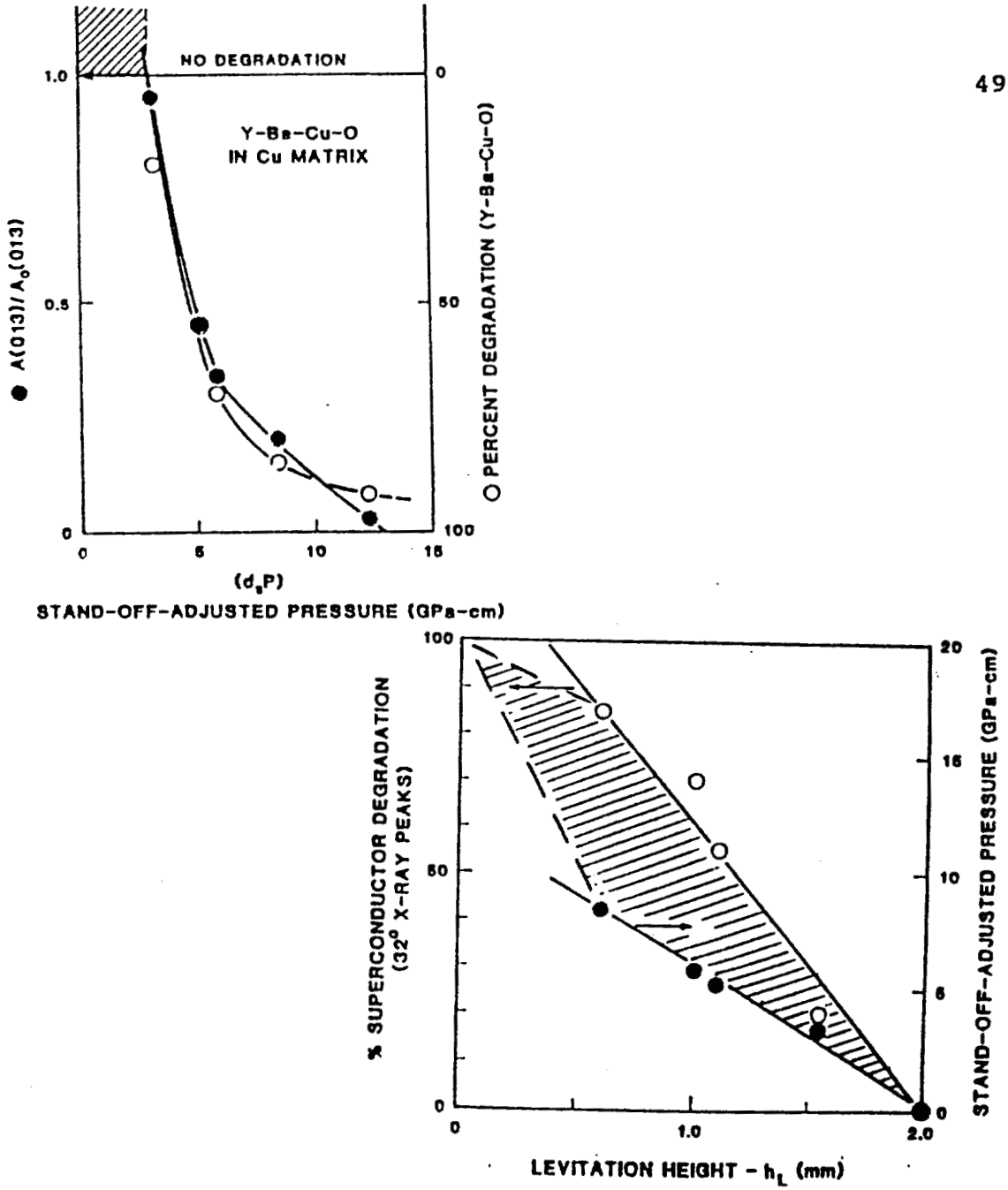

Figure 8a: Illustration of degradation in levitation height with percentage metal additions

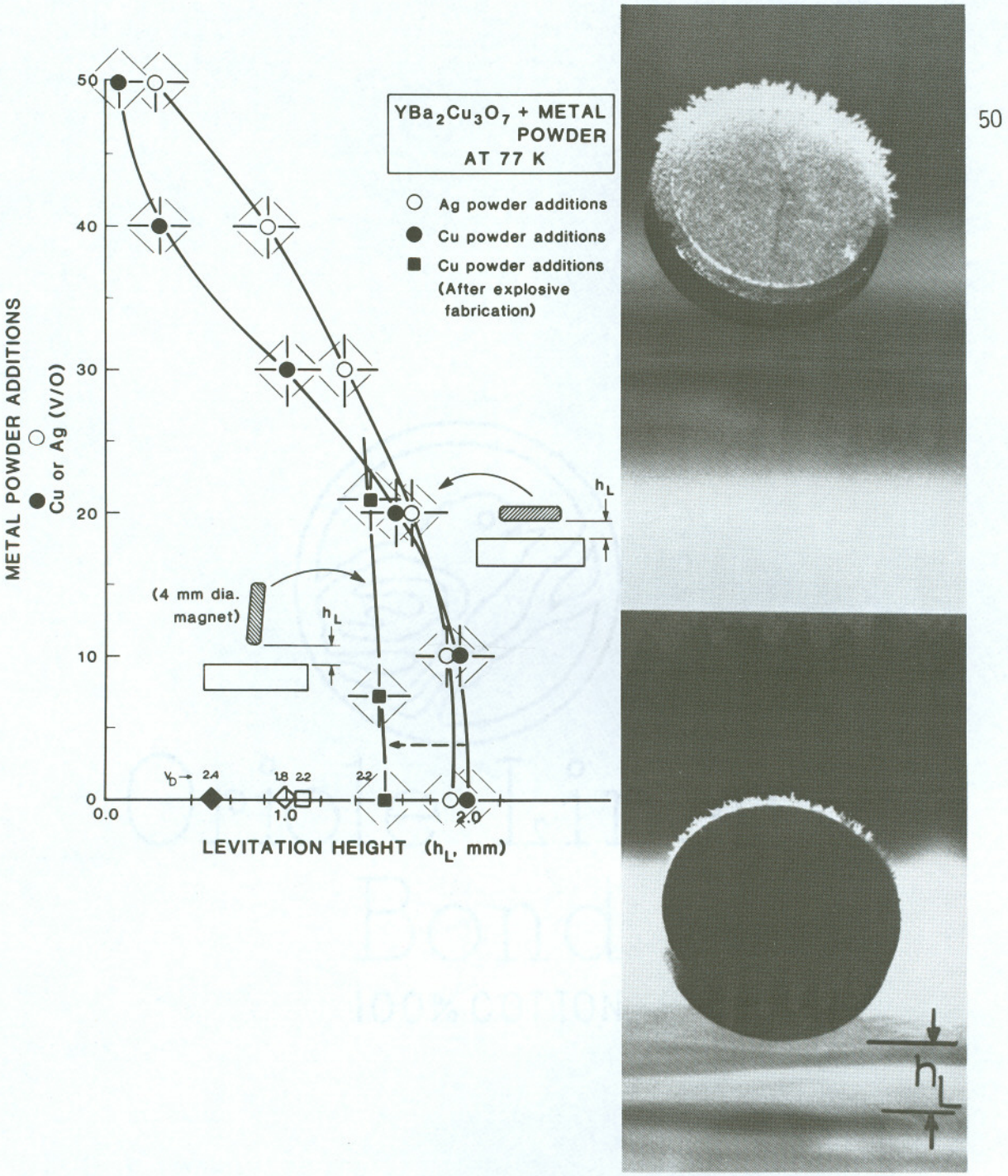

Figure 8b: Illustration of simple levitation height experiments with varying percentage of metal powder additions in $YBa_2Cu_3O_7$.

one was evacuated and the other assembly had no provision for vacuum.

The x-ray diagnosis revealed degradation. The x-ray split peak signatures indicated considerable peak height reductions and peak broadening shown in Figure (9). The degradation observed in this series was greater than that observed in Series one. In Series 2 the detonation velocity was 2.2 the same as Series 1 however the stand off distance was doubled d_s =.64cm and the peak pressure was 9 GPa. From the x-ray diagnosis it was clear that as the peak pressure increased the degradation increased. However more data was needed to confirm this result and owing to lack of data it was required to study the effect of higher pressures on degradation.

In addition it was also observed that there was no effect on degradation by evacuating the channels. Tooling plate A and B essentially yielded the same results (Figure 9 compare channel 1A and 1B). The x-ray split peak signatures were different between Series 1 and 2 because the experimental parameters had been modified. These parameters continued to be changed in an effort to eliminate degradation and develop a fabrication matrix.

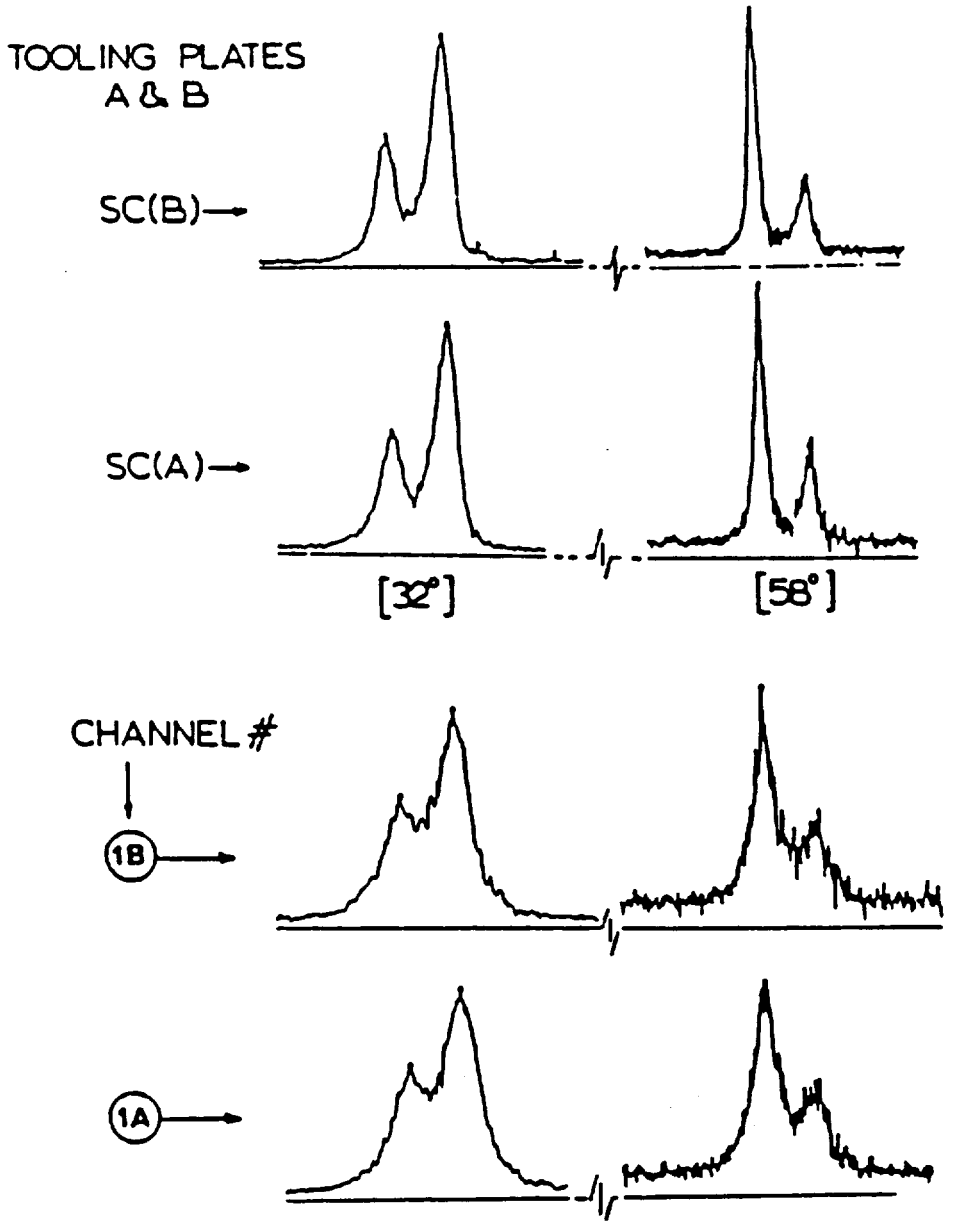

Figure 9 : X-Ray split-peak signatures for Y-Ba-Cu-O before fabrication SC and after fabrication in Series 2 experiments. The signatures show degradation of the superconductor in comparison to the starting powder.

It was understood that high peak pressure increases the theoretical density of the consolidated superconductor but at the same time degrades the superconducting properties (Figure 4a). However, various design modifications were carried out and in the Series 3, six experiments were carried out.

In 1.1 and 1.2 (vacuum) tooling plate designs the detonation velocity used was 1.8 Km/sec and the peak pressure used was 8 GPa. The x-ray data exhibited split peak signatures with peak reductions and peak broadening as illustrated in Figure 10. This degradation was less than that observed in Series 2. The split peak profile in Series 1 however showed less peak height reductions and peak broadening. No difference in the split peak profiles of 1.1 and 1.2 which had provisions for evacuation were observed.

The split peak signatures of 2.1 and 2.2 exhibited considerable peak broadening peak amplitude reductions. The split peak profiles were similar to those observed in Series 2. The V_d was 2.4 and peak pressure 13 GPa.

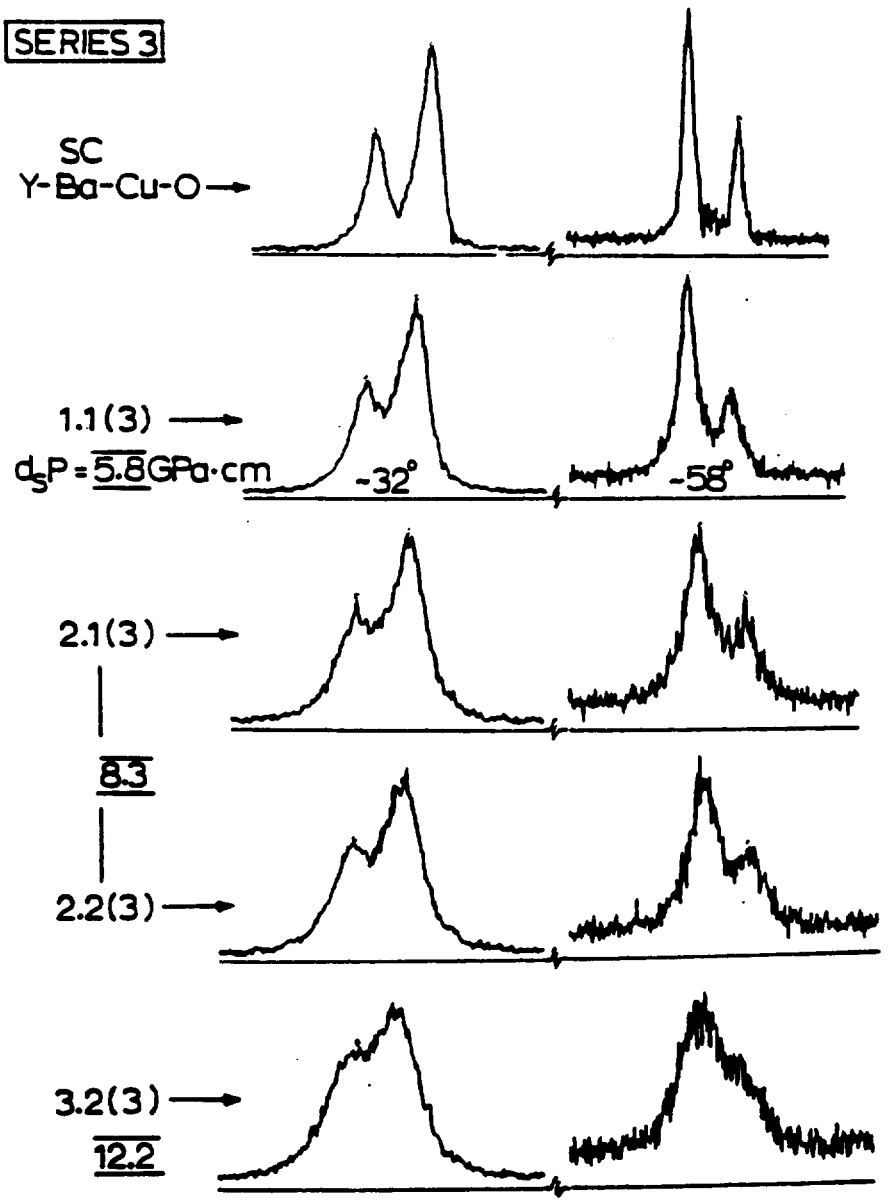

Figure 10: X-Ray split peak signatures for Y-Ba-Cu-O before fabrication and after fabrication in Series 3 experiments. The signatures show superconductor degradation with increasing values of dsP.

In Series 3.1 and 3.2 the two split peaks appeared to merge to form a single peak as illustrated in Figure 10. The detonation velocity was 2.9 Km/sec and the peak pressure 19 GPa. Thus, it was confirmed that at high peak pressures consolidation of the superconductor would yield highly degraded products. In addition higher peak pressures enhanced the theoretical density but promoted the formation of cracks and loss of superconducting properties. There existed a possibility that the shock wave induced some kind of degradation into the superconducting powders due to atomic displacements created in the shock front and this was pressure dependent. Thus these series necessitated that the pressures be minimized to minimize degradation without compromising the consolidation and welding efficiency.

The fabrication parameters were adjusted to produce lower peak pressures without compromising the welding integrity of the monolith. Thus in the Series 4 three series of experiments were carried out. The x-ray split peak signatures in the 4.1 series still exhibited peak height reductions and peak broadening as shown in Figure 11. However degradation revealed was much less than observed in Series 2 and 3.

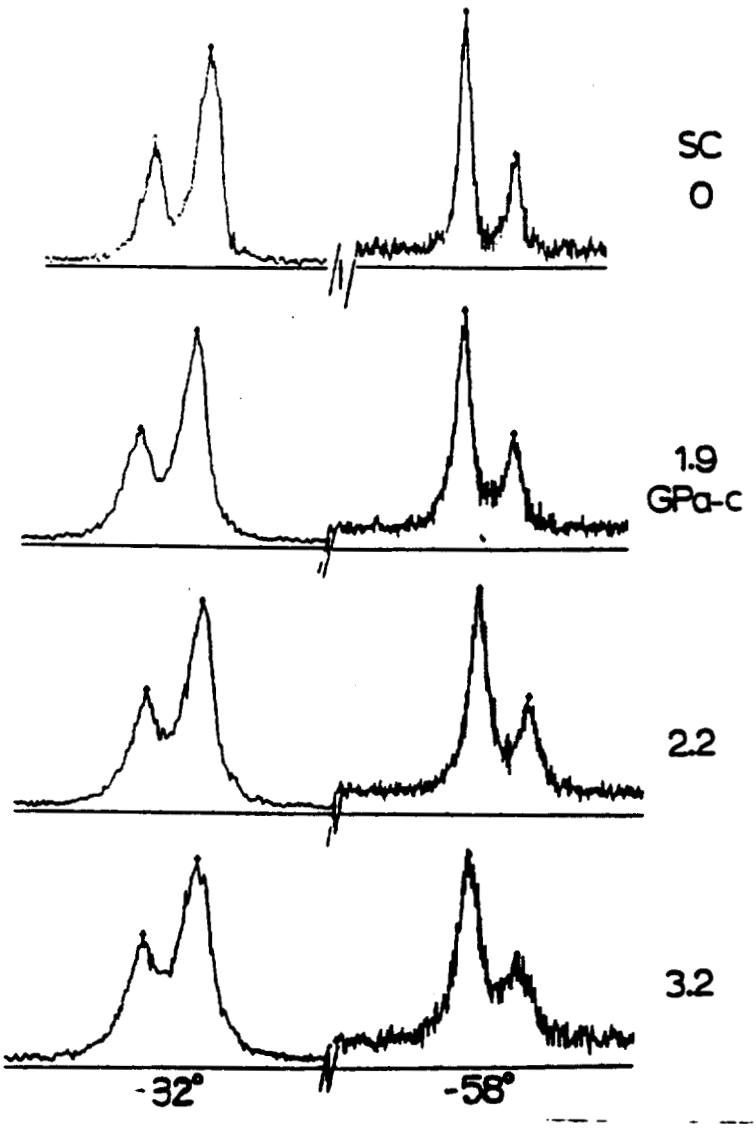

Figure 11: X-Ray split signatures (2θ = 32 and 58 degrees) for Series 4 experiments corresponding to peak pressures of 4, 5 and 7 GPa, respectively. It is evident 2θ=32 peak broadening increases with enhancing pressure.

In Series 4.1 the peak pressure used was 4 GPa and the detonation velocity used was 1.8 km/sec. In Series 4.2 the split peak pressure was 5 GPa and the detonation velocity 1.8 km/sec and in Series 4.3 peak pressure was 7 GPa and the detonation velocity 2 km/sec. The samples which were shocked to a peak pressure of 4 GPa revealed less peak broadening and peak height reductions than the split peaks observed in Series 2 and Series 3. In the Series 4 the degradation observed in the 4.1 series was less than that observed in the 4.2 and 4.3 samples. Thus it is evident that increase in shock pressure causes increase in degradation. This result is further confirmed by the data obtained from R-T curves.

R-T Curves

After shock processing, the R-T curves exhibit a semiconducting behavior in the normal state. However an important observation in the Tc onset for samples shocked between 4 and 13 GPa is the same as demonstrated by Figure 12a. These R-T signatures indicate broadening of the superconducting transition. Above 13 GPa the superconducting transition is annihilated and it has been shown by Murr et al [39], that a high temperature anneal above 900 C is

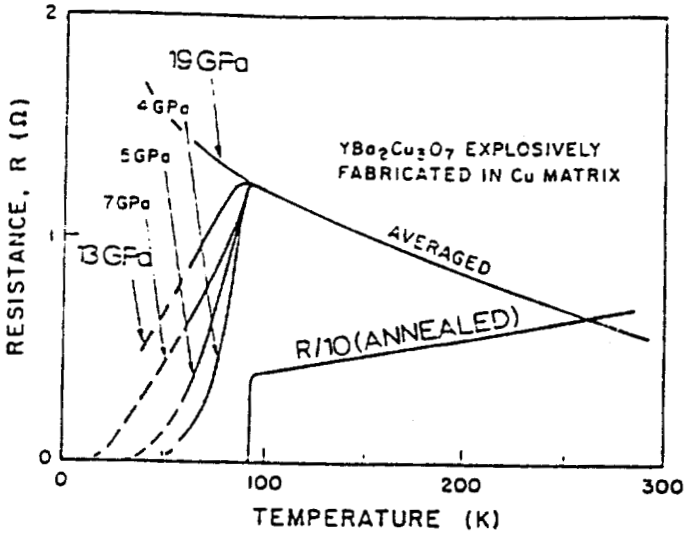

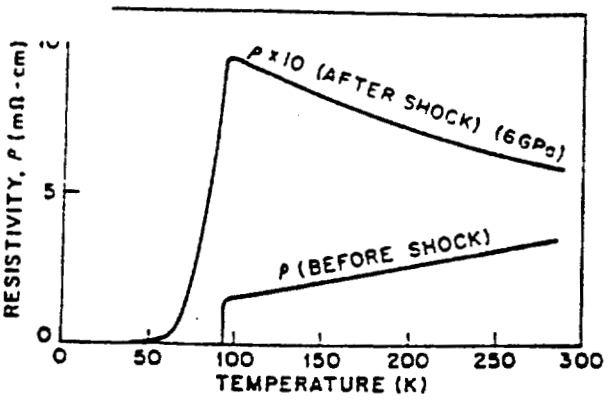

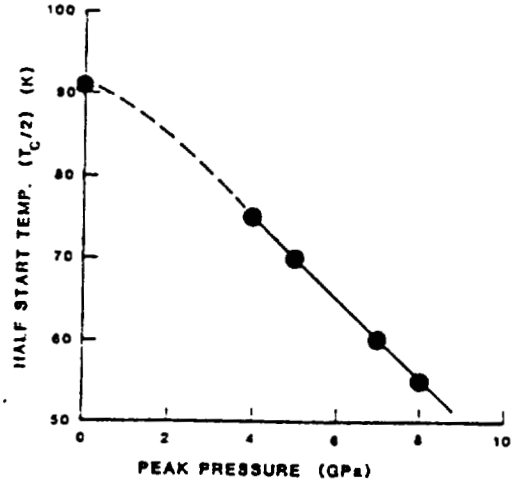

Figure 12: (a) Comparison of resistance-Temperature signatures for a range of explosively fabricated Y-Ba-Cu-O samples at different pressure. (b) R-T signatures of plane-wave loaded sintered bars. (c) Plot of T_c versus peak pressure.

essentially required to recover a sharp transition and a metallic R-T transition behavior in the normal state.

Figure 12a shows the R-T signatures indicating dramatic reductions in the zero resistance T_c values and in the sharpness of resistance (resistivity) temperature transition at peak shock pressures in excess of 15 GPa in explosively fabrication of $YBa_2Cu_3O_7$. In these samples no loss of oxygen has been observed by thermogravimetric analysis. These results are consistent with those observed in the x-ray analysis. This increase in broadening and eventually the destruction of the superconducting transition at higher pressures demonstrates the effect of shock pressures on superconductivity in $YBa_2Cu_3O_7$ inducing a semiconducting behavior in the normal state.

Figure 12b reproduces the results for plane-wave shock loaded sintered bars at 6 GPa. The results are consistent with and nearly identical to those shown in Figure 12a. These results demonstrate that the effects are due to the shock-wave and are not the result of particle heating, cracking or other features of the explosive fabrication process. Finally the broadening of the superconducting implicit in Figure 12a is

shown more recognizably by plotting the T_c (half-start) temperature as $T_c/2$ versus pressure in Figure 12 (c)

The fact that significant line broadening as well as systematic adjustments in specific peak reflections [013] and [213] occurs with increasing shock pressures is indicative of the fact that shock induced defects may contribute to the residual modified superconducting behavior.

MICROSTRUCTURAL OBSERVATIONS

The degradation observed in the superconductor stimulated great interest in their microstructure especially since the superconducting properties depend on parameters such as non-stoichiometry, phase composition, heat treatment and microstructure.

The specimens prepared for transmission electron microscopy were ion milled and highly vulnerable to decomposition. To prevent damage of the sample it was left in the vacuum of the ion milling equipment until it could be directly transferred into the electron microscope. The ion milled specimen degrades even if left in an evacuated desiccator and observed after 24 hours. A systematic study was done to observe the microstructural changes with changing peak pressures.

Figure 13 shows for comparison the starting superconducting $YBa_2Cu_3O_7$ powder morphologies and the coherent permutation interfaces which are characteristic of the orthorhombic, high T_c phase [40].

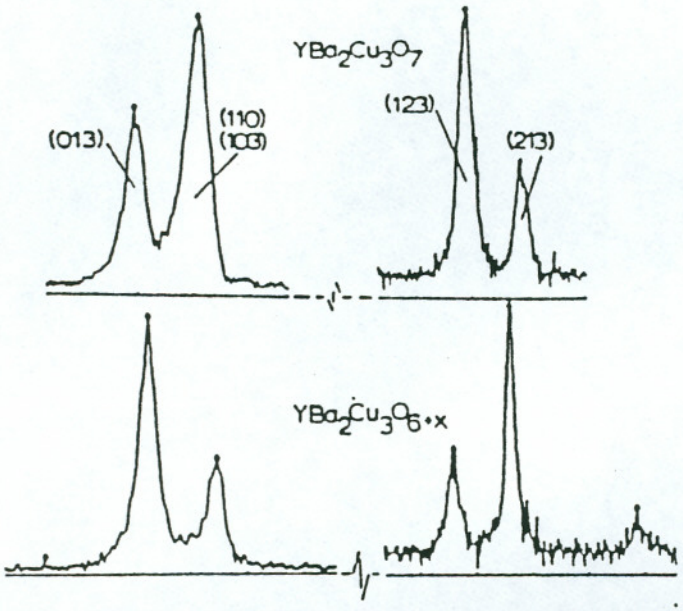

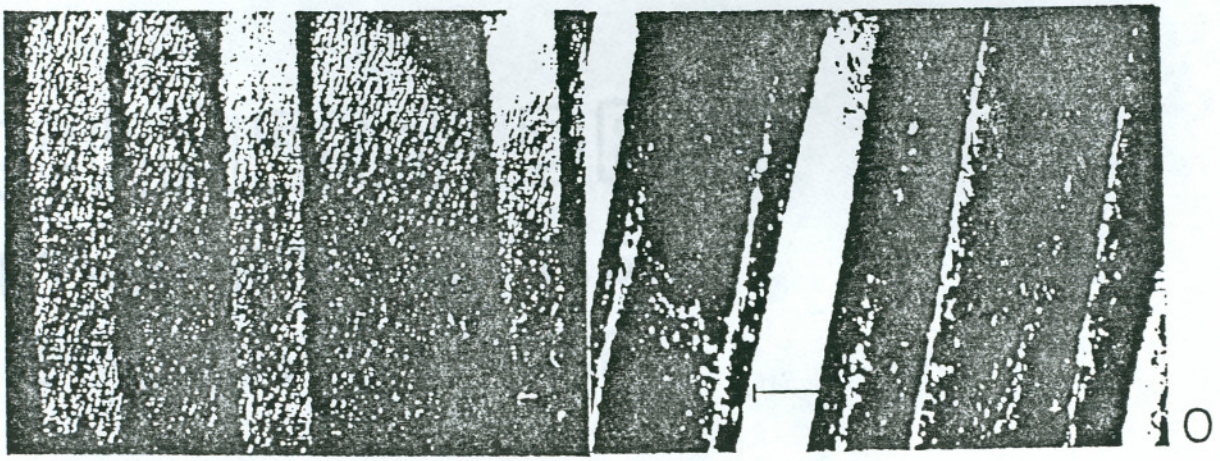

Figure 13: TEM (Bright field) images showing well defined twins in the starting powder and the x-ray split peak signatures.

In Series 1 the detonation velocity used was 2.2 km/sec and peak pressures 6 and 7 GPa. Figure 14 shows the microstructures of the shocked superconductor. In comparison to the unconsolidated and unshocked powder there is an increase in the twin density after explosive fabrication as well as an increase in dislocation density as shown in Figure 15a and b where the TEM images are compared with the x-ray split signatures for increasing, d_sP (GPa-cm) values. These microstructural changes are correlated with changes in characteristic split-peak signatures at $2\theta = 32$ and 58 degrees for the fabricated and encapsulated superconductors. The microstructural changes seemed to explain the cause for this degradation but at this stage it was too early to conclude if it was the twin density increase that was responsible for the degradation. Indeed these twins are produced by extremely small strains and are not representative of significant strain broadening in the X-ray peaks.

In an effort to improve upon consolidation and eliminate degradation and to achieve the required theoretical density in Series 2 the detonation velocity used was 2.2 km/sec and the peak pressures enhanced to 9 GPa by increasing the stand off distance to enable the flyer plate to acquire the required velocity for enhanced peak pressures. Figure 16 illustrates

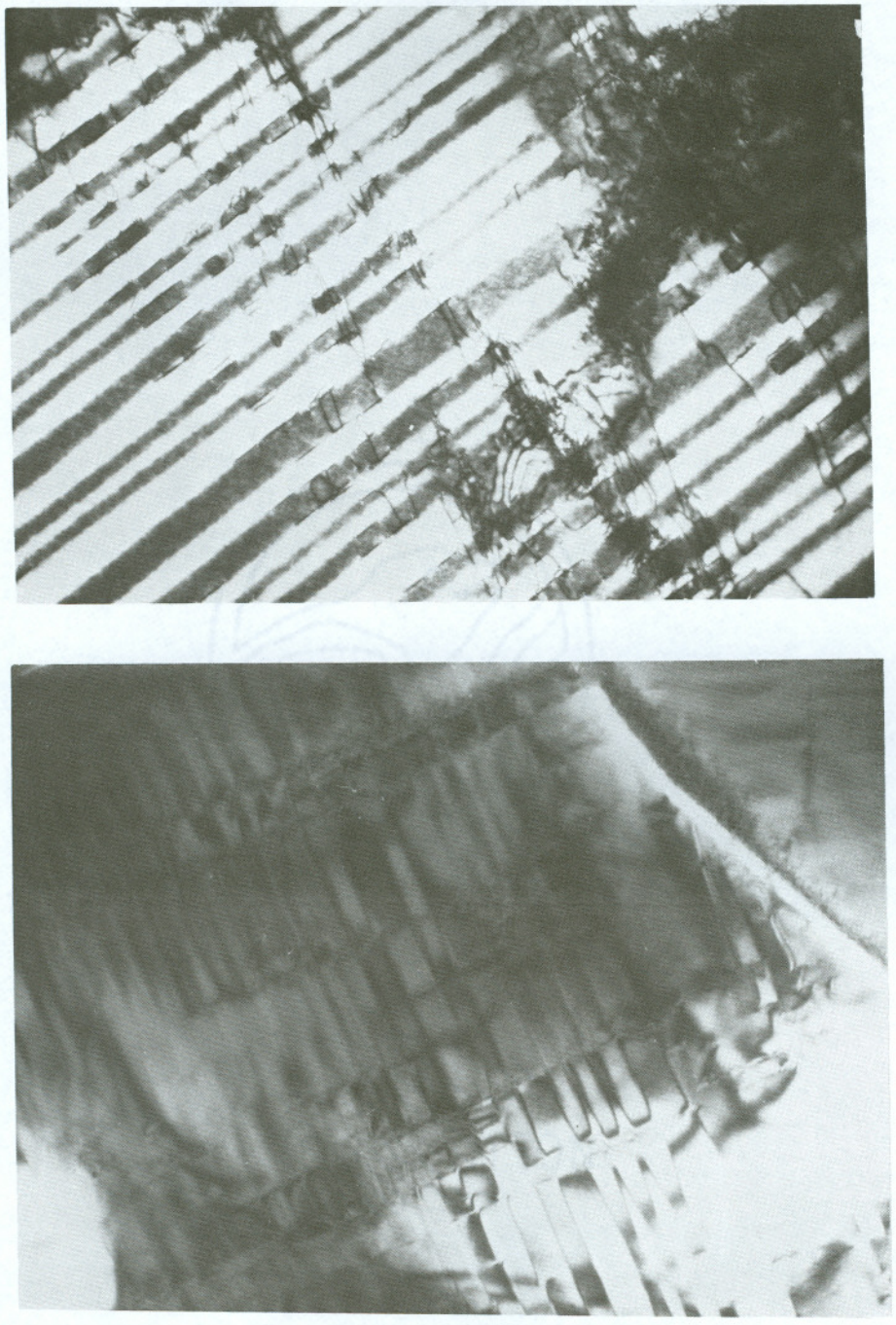

Figure 14: TEM micrographs showing increase in twin density and dislocation density in shocked superconductor (Series 1 7 GPa).

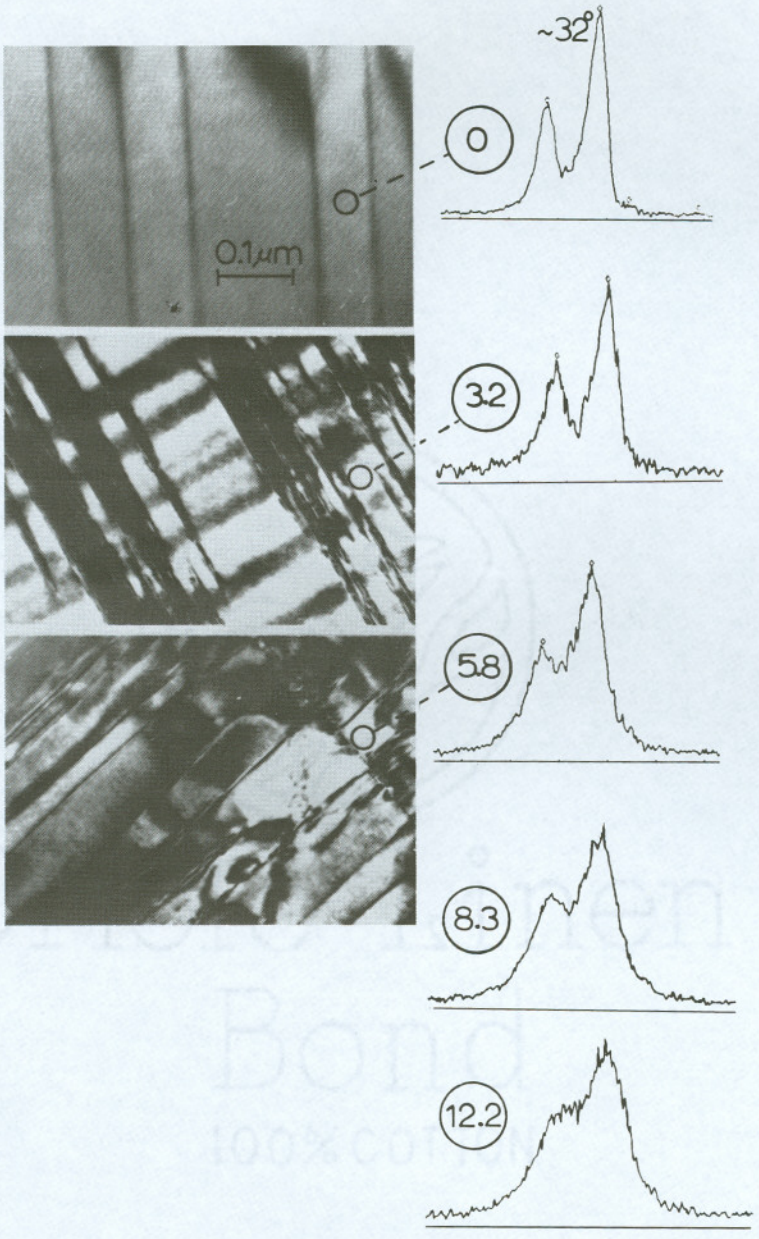

Figure 15a: TEM micrographs showing twin structures in Y-Ba-CuO and the corresponding x-ray split signatures.

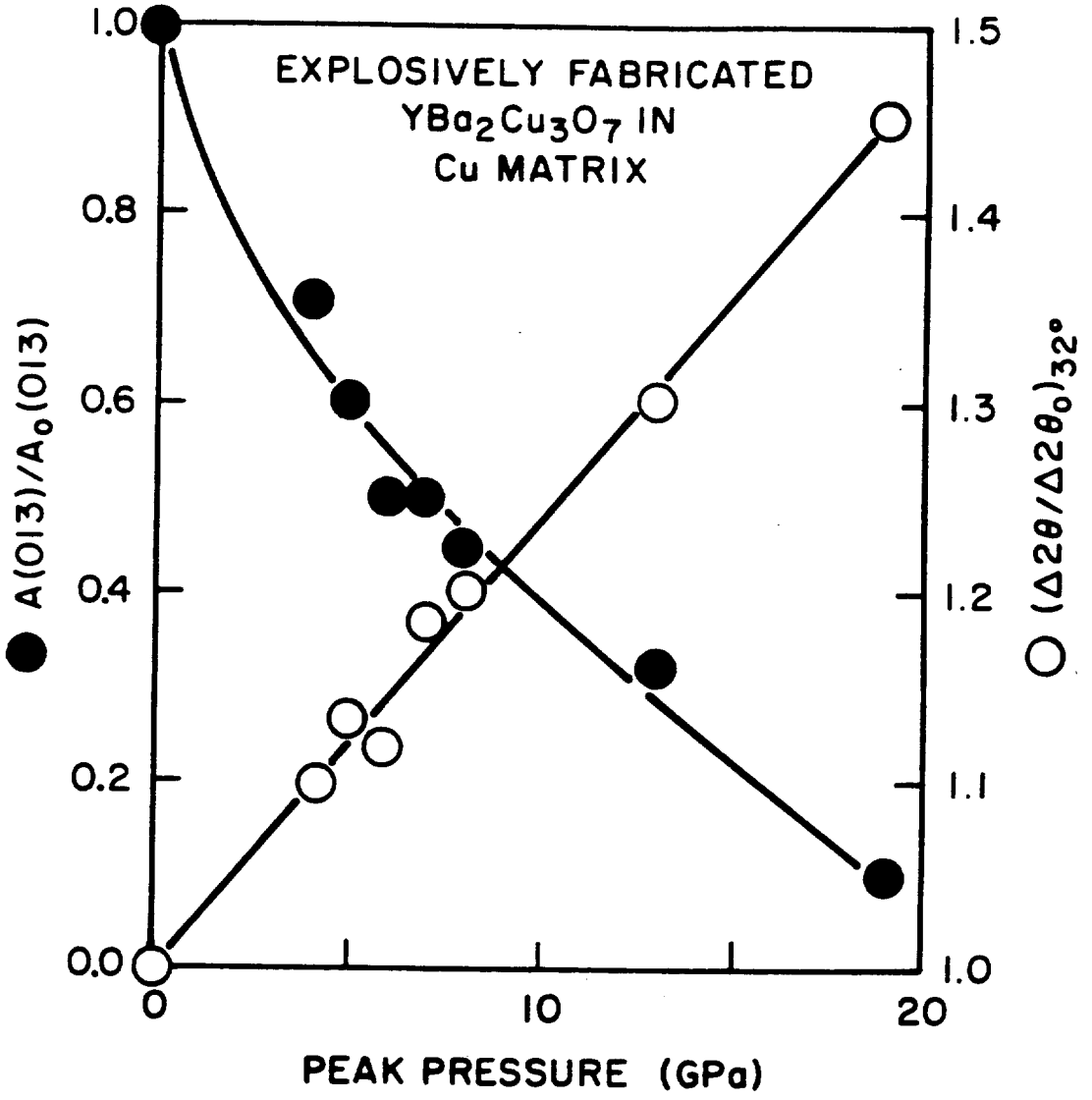

Figure 15b: Schematic illustration of increase in peak broadening ratio in explosively fabricated $YBa_2Cu_3O_7$ with increasing peak pressures.

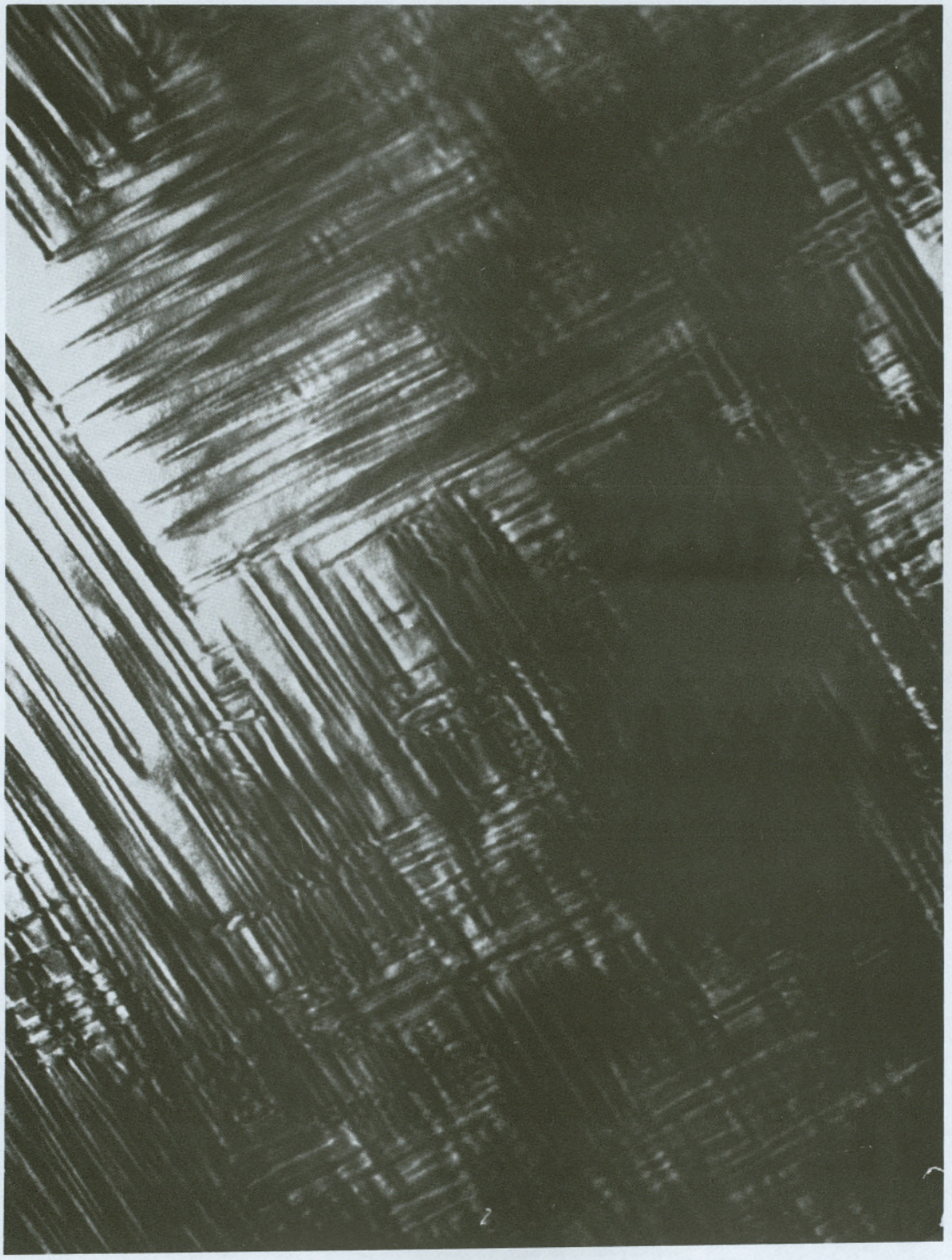

Figure 16: Microstructures observed in the Y-Ba-Cu-O samples

the microstructures observed. These microstructures revealed twins and heavy dislocation density. However in comparison to Series 1 it was hard to distinguish whether there was an increase in twin density, since the twins were highly tilt sensitive. In comparison to the starting powder it was clear that new twins different from the ones observed in the starting unshocked powder had appeared as shown in Figure 15.

However Deutcher and Muller [41] have contended that "internal Josephson junctions " at twin boundaries within individual grains also contribute to diminished super current. H.W.Zandbergen and G.Thomas [42] have stated that the twins are formed during the formation of the tetragonal crystal and are not formed due to impinged grain growth.

It was apparent that there was a considerable increase in twin density but it was too early to attribute the degradation entirely due to enhancement in twin density. It has also been shown by Murr et al that the metallic superconductor behavior is not observed in the superconductor until post fabrication annealing exceeds 700C. Twins are annealed out at much lower temperatures.

In Series 3 more dense shear type planar defects were observed at the maximum fabrication pressure (19 GPa) in the transmission electron microscope where the density of microtwins appeared to decline from those observed at lower pressures and their nature changed.

A tilt sensitive mottling appeared to override the microstructural background, often giving rise to dense clusters, "loops" or precipitate-like features which were associated with the planar shear defects and dislocations as shown in Figure 17.

In Series 4 low pressures were used, the x-ray analysis revealed much less degradation than that observed in the high pressure series. The split peak signatures exhibited decreased (013) amplitude peak broadening than observed in the high pressure series. Examination of samples at lower pressures also illustrated loops or precipitate-like features which were associated with planar shear defects which were characteristic of all shock fabricated materials, including shock loaded, sintered Y-Ba-Cu-O.

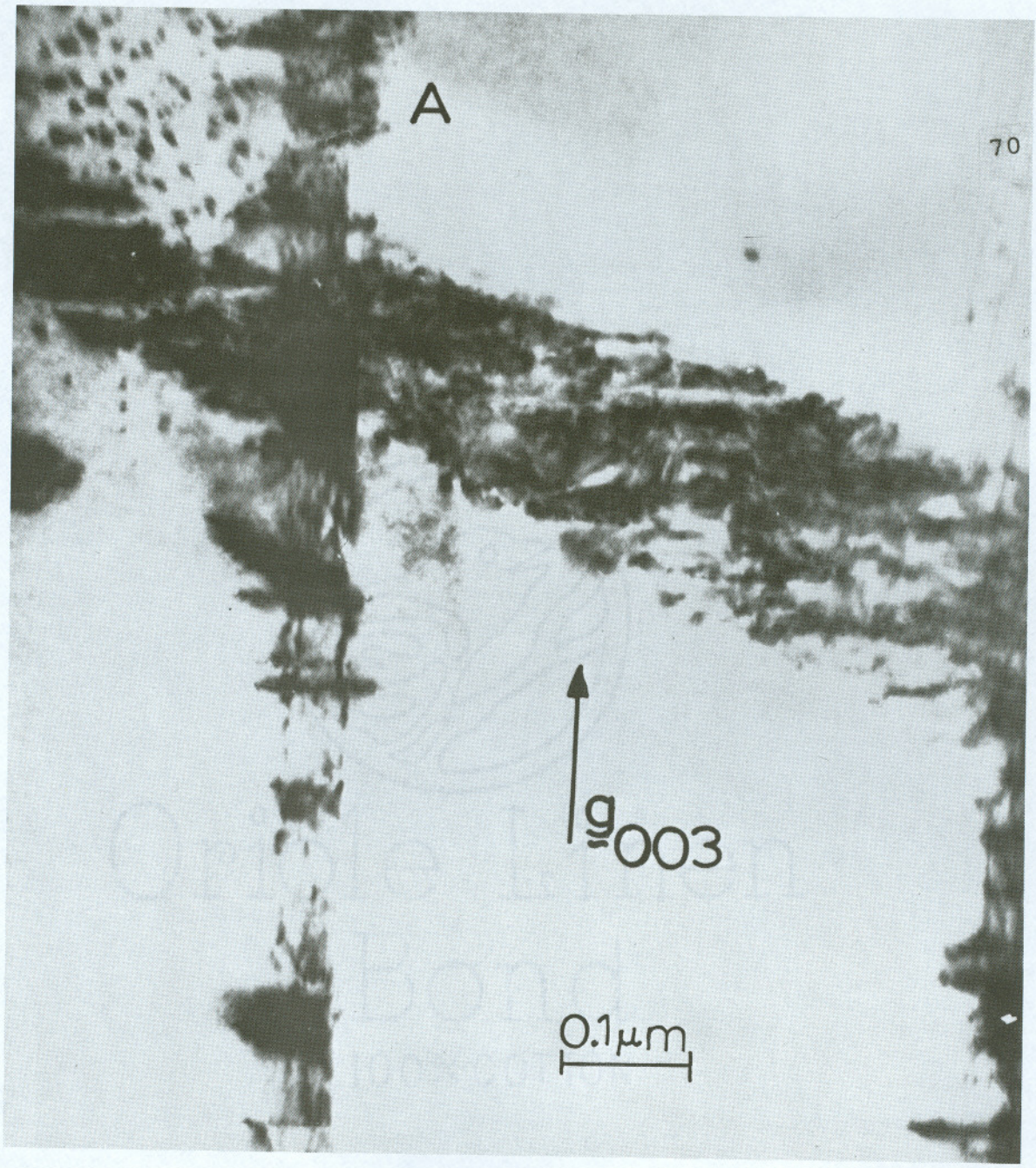

Figure 17: Bright-field diffraction contrast image showing shear-band like planar defects and dislocations decorated with clusters or precipitate like defects which also appear in region A after explosive fabrication of YBaCuO at 19 GPa peak pressure.

Detailed studies revealed the precipitate-like defects shown in Figure 18 to be localized lattice distortions exhibiting a different structure from the YBaCuO, which create local lattice strain as shown in the lattice-resolved diffraction contrast in the bright-field image shown in Figure 19. A variety of shear-type and planar defects as well as order-disorder phenomena have been reported [17,18]. These defects have also been observed in the plane wave shocked sintered bars Figure 20.

A model of the [010] fringe splitting which characterizes the local structure changes is shown in Figure 21. A detailed study of these defects revealed that some of the fringes are observed to be splitting or distorted throughout some regions as if a displacement-related, polytypic regime is created as a precursor to the defect-structure localization shown in Figure 21. Preliminary examinations in explosively fabricated Y-Ba-Cu-O specimens using weight loss comparisons have indicated little, if any, oxygen loss up to 8 GPa, and previous, comparative thermogravimetric analysis of unshocked and plane-wave shock loaded dense, sintered $YBa_2Cu_3O_{6.9}$ also indicated no oxygen loss.

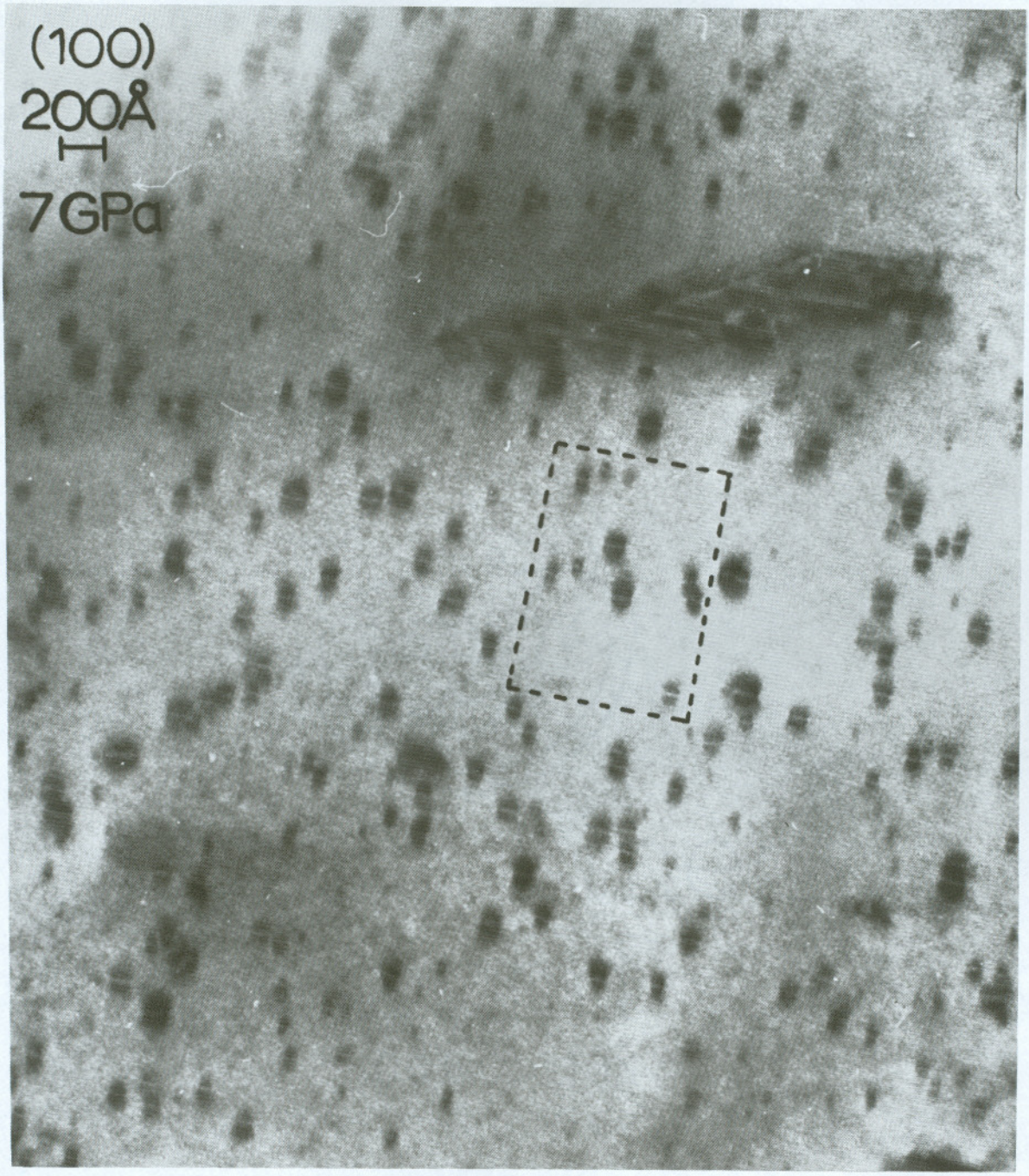

Figure 18: Bright-field diffraction contrast and lattice image sequence showing localized lattice defects in explosively fabricated $YBa_2Cu_3O_7$ (at P = 7 GPa). Low magnification image showing strain-field contrast.

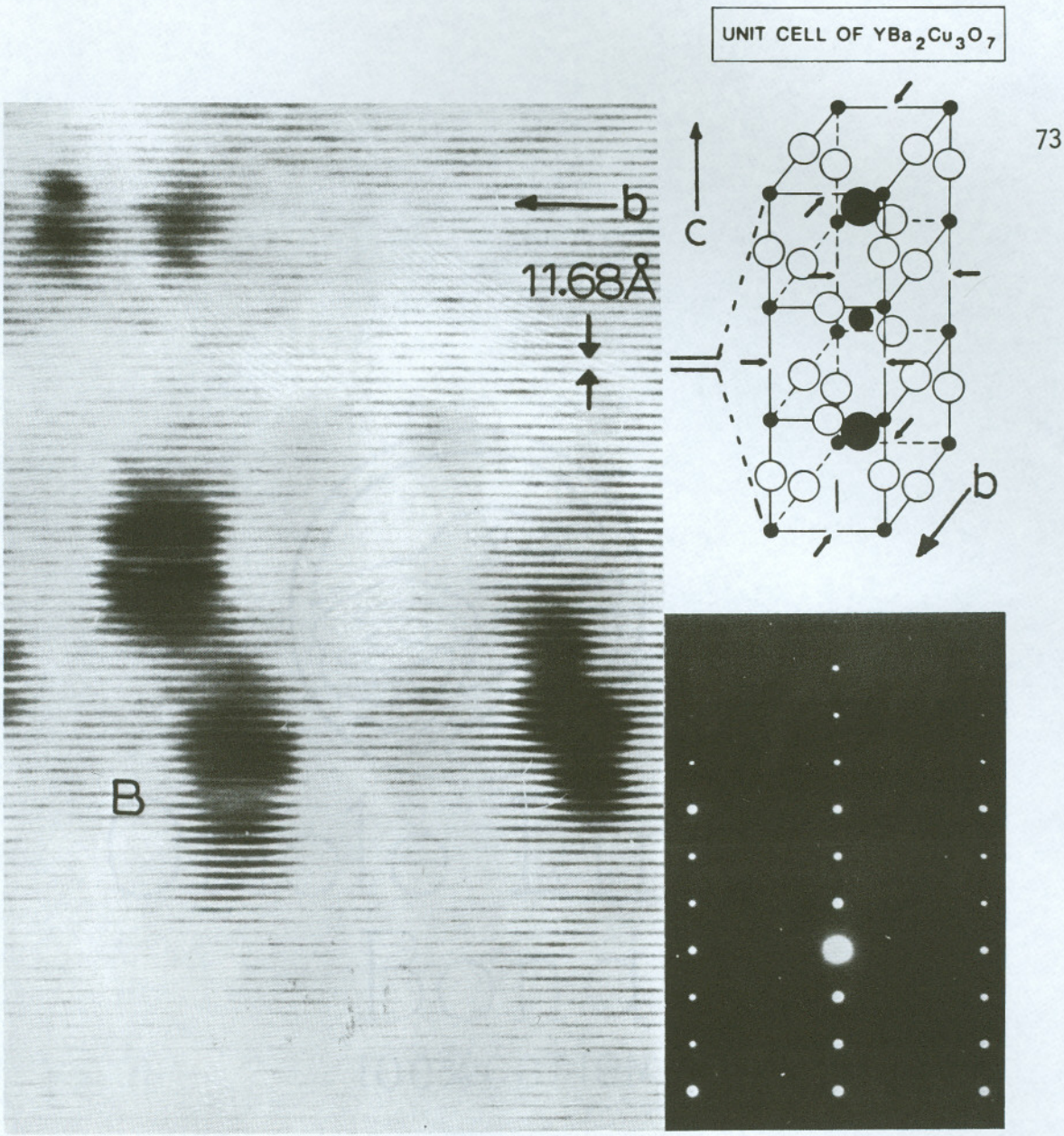

Figure 19: Higher magnification of area dotted in Figure 18 showing localized zones of [010] fringe splitting within the strain-field contrast regimes. The corresponding electron diffraction pattern illustrates the [100] zone to be the viewing direction corresponding to the idealized unit cell a-direction.

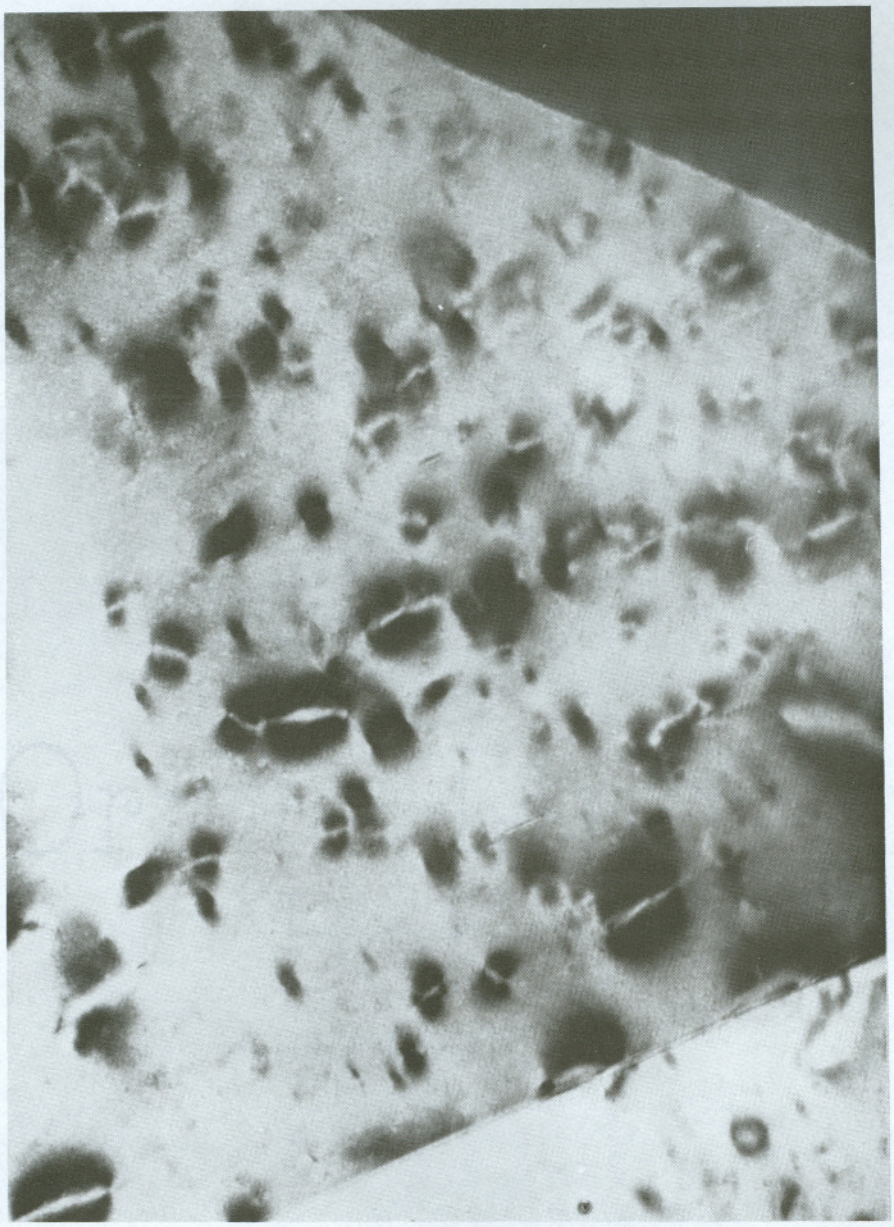

Figure 20: Bright-field diffraction contrast and lattice image sequence showing details of localized lattice defects in plane-wave shock loaded Y-Ba-Cu-O sintered bars.

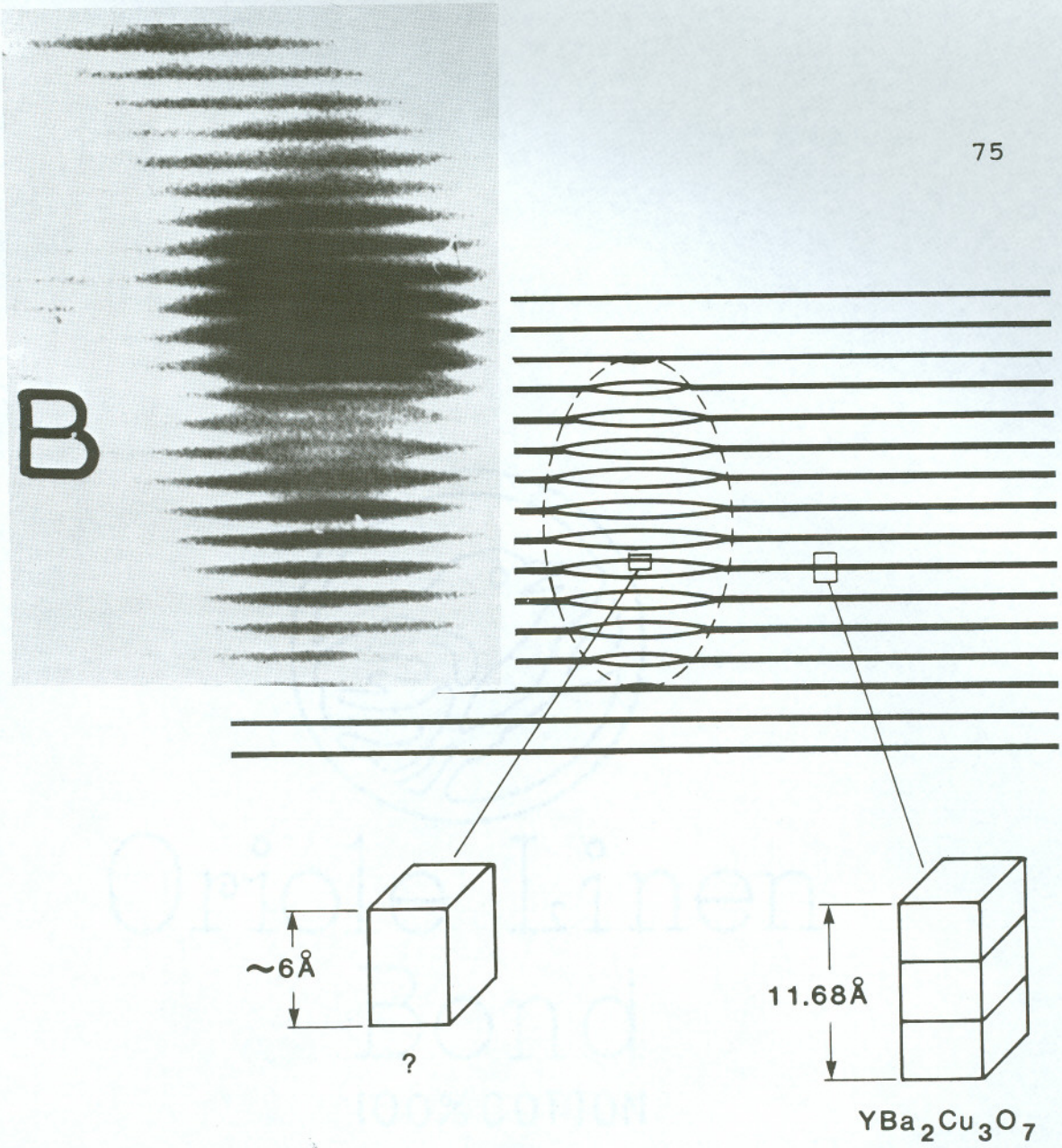

Figure 21: Enlarged view and contrast comparison of defect at B in Figure 18 along with a schematic view clarifying the localized regime to be a different crystal structure with c=6A or c/2 for the Y-Ba-Cu-O unit cell.

Since loss of other metallic elements is even more unlikely, the degradation shown by x-ray analysis and R-T curves can be attributed as a shock wave induced disorder. Figure 21 shows distortion of the fringes which could be attributed due to displacements of Y,Ba,Cu or oxygen atoms however simple oxygen displacements should allow rapid rearrangement and restoration of superconductivity at relatively low annealing temperatures.

These features have not been observed in the unshocked, unfabricated powders or the unshocked sintered bars of $YBa_2Cu_3O_7$ prepared and observed under identical conditions and thus they may be primarily responsible for the unique, degradation-related behavior of explosively fabricated and shock loaded Y-Ba-Cu-O. These localized defects explain the degradation observed in the x-ray spectrum and resistance-temperature curves. The decline in the (013) amplitudes represents a loss of long range structural order while the increase in peak broadening is indicative of increasing internal nonuniform lattice strain or characteristic increases in shock-induced crystal defects as illustrated in the Figures 18 to 21. These defects also exhibit large strain fields shown by the black contrast lobes and these strain field are phenomenologically the same as the broadened peaks in the x-ray diffraction signatures.

CHAPTER 5

SUMMARY AND CONCLUSIONS

In the present study efforts have been directed towards evaluating, the effects off explosive fabrication on the residual superconductivity of $YBa_2Cu_3O_7$.

Superconducting properties have been found to degrade with increasing peak pressures. This degradation is exhibited by the peak broadening and reduced peak heights observed in the characteristic orthrhombic split peak signatures at 2θ = 32 and 58 degrees.

The residual superconductivity determined by the R-T signatures also exhibited systematic degradation with increasing shock pressures. Although no sharp transition was observed in the R-T signatures of the fabricated superconductor, however the T_c onset was unchanged for peak shock pressures less than 13 GPa. In addition the superconducting transition is broadened as the peak pressure is increased.

Significant line broadening and peak height reductions and transition broadening occur with increasing peak pressures is indicative that shock induced defects contribute to the degradation in superconducting properties.

The observation of cluster-like-defects in transmission electron microscopy, associated with large elastic strain fields accounts for the degradation in superconductors. It has also been observed that these defects increase with increasing peak pressures. These defects have also been observed in plane-wave shock loaded sintered materials which also show degradation in superconducting properties after subjecting them to a plane shock wave creating a peak shock pressure of 6 GPa.

Thus the annihilation of superconducting properties is not simply the result of orthrhombic to tetragonal structure transformation but due to microstructural transformation induced by the shock wave.

REFERENCES

1 H.K. Onnes, Commun. Kammerlingh Onnes Lab. Univ. suppl.346 (1913).

2 J.G. Bednorz and K.A.Mueller, Z.Phys., 863, 189 (1986).

3 C.W. Chu, P.H.Hor, R.L. Meng, L. Gao, Z.J. Huang, Science, **235**, 567 (1987).

4 C.W. Chu et al., Nature, **331**, 377 (1988).

5 A.W. Sleight, J.L. Gilson, P.E. Bierdsteddt, Solid State Comm., **17**, 299 (1975).

6 B.T. Matthias, T.H.Geballe, S. Gellar, E. Corenzwit, Phys.Rev., **95**, 1435

7 J. Bardeen, L.N. Cooper, J.R. Schrieffer, Phys. Rev. **108** (1957).

8 H. Maeda et al.,Nature, **331**, 377 (1988).

9 I.K. Schuller, J.D. Jorgensen, MRS (1989).

10 J.D. Jorgensen, Jpn. J. Appl. Phys. **26** (1987).

11 M.A. Beno et al, Appl. Phys.Lett. **51** (1987).

12 H. Takagi, S. Uchida, K. Kitazawa, S. Tanaka, Jpn. J. Phys. **26** (1987).

13 J.D. Jorgensen, H-B. Schuuttler, D.G. Hinks,D.W. Capone II, K. Zhang, M.B. Drodsky, D.J. Scalapino, Phys. Rev. Lett. **58** (1987).

14 M.B. Maple, Y. Dalichaouch, J.M. Ferreira, R.R. Hake, B.W. Lee, J.J. Neumeier, M.S. Torikachvili, K.N. Yang, H. Zhou, R.P. Guertin, M.V. Kuric, Physica B **148** (1987).

15 T.P. Orlando, K.A. Delin. S. Foner, E.J. McNiff, Jr., J.M. Tarascon, L.H. Greene, W.R. McKinnon, G.W. Hull, Phys. Rev. B **36** (1987)

16 J.J. Neumeier, Y. Dalichaouch, J.M. Fereira, R.R. Hake, B.W. Lee, M.B. Maple, K.N. Yang, R.P. Guertin, M.V. Kuric, Physica C **152** (1988).

17 Robert B. Laibowitz MRS, XIV, **1** (1989).

18 S. Tanaka, H. Itozaki, Jpn. J. of Appl. Phys. **27** (1988)

19 K.P. Staudhammer, L.E. Murr 'Shock waves for industrial applications'

20 L.E. Murr, S. Shankar, A.W. Hare, K.P. Staudhammer, Scripta Met.,**17**, 1353 (1983)

21 A.W. Hare, L.E. Murr, F.P. Carlson, U.S. Patent #4, 490, 329, Dec. 25 (1984).

22 L.E. Murr, A.W. Hare, N.G. Eror, Nature (London) 329, 37 (1987).

23 L.E.Murr, A.W. Hare, N.G. Eror, Adv.Mater. Processes 132, 36 (1987).

24 W.J.M. Rankine, Phil. Trans. Roy. Soc. (London), 160 (1870)

25 J.Hugoniot, J. Ecole Polytech, 58 (1889).

26 L.E.Murr 'Shock Waves For Industrial Applications' 1989.

27 M. Rice, R.G. McQueen, J.M. Walsh, Compression of Solids by Strong Shock Waves, Solid State Physics, Vol. 5, Academic Press, New York (1958).

28 M.A. Meyers, L.E. Murr Eds., 'Shock- waves and High-Strain Rate Phenomenon in Metals',Plenum Press, New York (1981).

29 L.E. Murr, K.P. Staudhammer, M.A. Meyers, Eds., 'Metallurgical Applications of Shock-Wave and High-Strain-Rate-Phenomena,Marcel Dekker', New York (1986).

30 N.V. Naumovich, Powder Metallurgy Assoc. of Byelorussian Republic, Minsk, USSR, private communication (1985).

31 S. Saito, A.B. Sawaoka, Proc. 7th AIRAPT Conference, High Pressure Science ad Technology, Le Creusot, France (1979).

32 W.H. Gourdin, Prog. in Materials Science, 30, 39 (1989)

33 "Dynamic Compaction of Metaland Ceramic Powders " NMAB 394,National Materials Advisory Board, National Academy of Sciences (1983).

34 G.R. Cowan, O.R. Bergmann, A.H. Holtzmab, Met.Trans., 2, 3145 (1971)

35 V. Shribman, A.S. Bahrani, B. Crossland, Prod. Engr. (1969).

36 T.Z. Blazynskii, Ed., 'Explosive Welding, Forming and Compaction', Applied Sciences Ltd. New York (1983).

37 J.S. Rinehart and J. Pearson, 'Explosive Working of Metals', Press, New York (1963).

38 L.E. Murr, T. Monson, M. Strasik, U. Sudarsan, N.G.Eror, A.W. Hare, D.G. Brasher, D.J. Butler, J. Metals 40 (1), 19 (1988).

39 Murr et al, Appl. Phys. Lett. 35, 1595 (1989).

40 G. Van Tendeloo, H.W. Zandbergen, and S. Amelinckx, Solid State Commun. 63, 389 (1987).

41 G.D. Duetcher and K.A. Mueller, Phys. Rev. Lett. 59, 1745 (1987).

42 H.W. Zandbergen, G. Thomas, Phys Stat.sik, 107, 825 (1988).